

Quantum Enhanced Precision Estimation with Bright Squeezed Light

G. S. Atkinson,^{1,2,*} E. J. Allen,^{1,†} G. Ferranti,¹ A. R. McMillan,¹ and J. C. F. Matthews^{1,‡}

¹*Quantum Engineering Technology Labs, H. H. Wills Physics Laboratory and Department of Electrical & Electronic Engineering, University of Bristol, Tyndall Avenue, BS8 1FD, United Kingdom.*

²*Quantum Engineering Centre for Doctoral Training, H. H. Wills Physics Laboratory and Department of Electrical & Electronic Engineering, University of Bristol, Tyndall Avenue, BS8 1FD, United Kingdom.*

(Dated: August 21, 2022)

Squeezed light has lower quantum noise in amplitude or phase than the quantum noise limit (QNL) of classical light. This enables enhancing sensitivity — quantified by the signal-to-noise ratio (SNR) — to beyond the QNL in optical techniques such as spectroscopy, gravitational wave detection, magnetometry and imaging. Precision — the variance of repeated estimates — has also been enhanced beyond the QNL using squeezed vacuum to estimate optical phase and transmission. However, demonstrations have been limited to femtowatts of probe power. Here we demonstrate simultaneous precision and sensitivity beyond the QNL for estimating modulated transmission using a squeezed amplitude probe of 0.2 mW average (25 W peak) power. This corresponds to 8 orders of magnitude above the power limitations of previous sub-QNL precision measurements. Our theory and experiment show precision enhancement scales with the amount of squeezing and increases with the resolution bandwidth of detection. We conclude that quantum enhanced precision in estimating a modulated transmission increases when observing dynamics at \sim kHz and above. This opens the way to performing measurements that compete with the optical powers of current classical techniques, but have superior precision and sensitivity beyond the classical limit.

Optical measurements are fundamentally limited by quantum fluctuations in the probe. The Poisson distributed photon number n of coherent light — often used as a probe in classical experiments — results in shot-noise, which represents the QNL in the precision of parameter estimation with classical resources [1]. Because the QNL scales with $\sim 1/\sqrt{n}$, longer measurements and higher intensity can increase precision. We may also increase precision with more interaction between probe and sample via multiple passes [2, 3] or optimising sample concentration [4]. However, there can often exist restrictions on the total optical exposure, the measurement time and sample concentration [5]. By using non-classical light, the fluctuations in the probe can be reduced below the QNL, thus providing ‘sub-shot-noise’ precision per photon [6]. The QNL defines the best precision achievable without the use of quantum correlations for a given apparatus and photon number [7]. This is distinguished from the standard quantum limit (SQL), which defines a measurement-independent limit to the precision that may be achieved using a minimum uncertainty state of a given photon number, without quantum resources [8]. Because squeezed light can offer significant reduction in noise below the QNL [9], and can be generated with arbitrary intensity using coherent laser light [10], it offers a practical approach for enhancing optical techniques beyond classical limitations.

Precision in measuring a parameter can be quantified by the inverse of the variance of corresponding measurement outcomes, and is bounded by the Fisher information according to the Cramér-Rao bound [11]. By contrast, the sensitivity of a measurement is the smallest possible signal that may be observed [12], and thus depends only on the signal-to-noise ratio (SNR). Photonic (definite photon number) quantum metrology [13] uses photon counting to observe quantum correlations between modes to reduce the noise of a measurement [13–15]. Here one can attain a quantum advantage in

both precision and sensitivity, by improving the Fisher information and reducing the optical noise floor. However, due to limitations in both the maximum photon flux and detector saturation power, the probe powers achievable are in practice $\mathcal{O}(10^6)$ photons detected per second (fW) [13, 14], which limits use to only cases that are reliant on ultra low intensities. Homodyne detection of squeezed vacuum has been used to estimate phase with sub-QNL precision [16, 17]. This is possible because measurement is performed away from low frequency technical noise, in a shot-noise limited bandwidth where squeezing reduces vacuum noise. However, as with photonic quantum metrology, strategies using squeezed vacuum for sub-QNL precision have also been restricted in maximum optical probe power.

Measurements using high power squeezed light can reach sub-QNL sensitivity in detection of phase modulation [6] and amplitude modulation (AM) [18]. This is because modulation introduces AC components in the detected signal, which can be made to coincide with a shot-noise-limited detector bandwidth, while squeezed light reduces the optical noise relative to the signal. The sensitivity of any frequency domain measurement of an optical signal in a shot-noise limited bandwidth may be improved by such techniques and this has been demonstrated in a range of applications (e.g. [7, 19–23]). However, enhancing sensitivity is not a sufficient condition to enhance precision. When bright optical probes are used, the noise in the bright field often dominates over the vacuum noise, which prohibits the use of squeezed light for reaching precision beyond the QNL. For squeezed light to provide a precision improvement in such a measurement, the variance of the measured signal must be limited by optical shot-noise. Here, we fulfill this condition and use bright amplitude squeezed light to measure AM with precision beyond the QNL.

The parameter of interest here is the modulation index

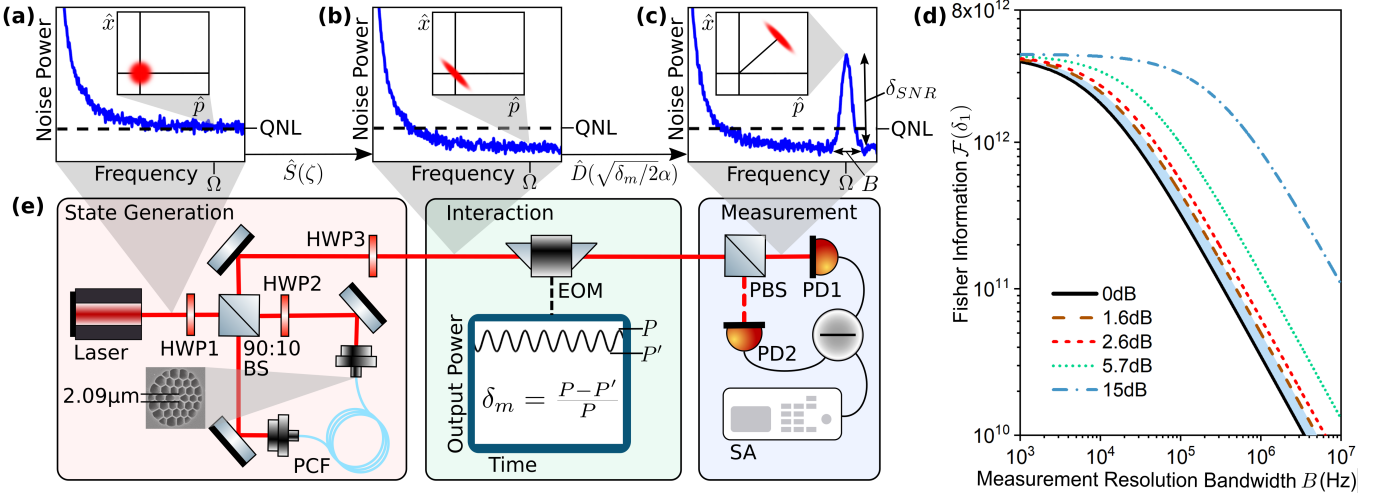


Figure 1. Modelling enhanced precision measurement of AM, and experimental setup. (a-c) Plots of spectral noise power illustrating the effect of amplitude squeezing and modulation on a typical laser source, with the quadrature diagrams showing a coherent state defined by \hat{x} , \hat{p} at $\pm\Omega$. (d) Theoretical model of the Fisher information $\mathcal{F}(\delta_m)$ for a coherent state (solid line) and squeezed states (dashed lines): -1.6 dB and -2.6 dB are the measured and inferred generated squeezing levels in our experiment, -5.7 dB is amplitude squeezing previously achieved using an asymmetric Kerr interferometer [24] and -15 dB is the highest measured squeezing to date [9]. For each plot, $P = 0.2$ mW, $\lambda = 740$ nm, $\eta = 1$, $\delta_m = 1 \times 10^{-4}$, $\text{Var}(\mathcal{H}) = 1 \times 10^{-4}$ and $\text{Cov}(\mathcal{H}_0, \mathcal{H}) = 1 \times 10^{-2}$. (e) Schematic of the experiment and SEM image representative of the PCF structure. A pulsed laser at 740 nm propagates into the Sagnac interferometer for squeezed state generation. A birefringent photonic crystal fibre (PCF) provides the nonlinear medium for Kerr squeezing. The electro-optic modulator (EOM) combined with the polarising beamsplitter (PBS) are used to generate AM, which is measured on a spectrum analyser (SA).

$\delta_m = (P - P')/P$, where P and P' are the maximum and minimum output power transmitted through a modulated loss (fig. 1(e)) [1]. For modulation frequency Ω , sinusoidal AM generates optical sidebands at $\pm\Omega$ from the carrier frequency. Upon photodetection, this leads to a single electronic sideband in the spectral noise power at frequency Ω that contains information about δ_m . Fig. 1(a-c) illustrate the behaviour of the spectral noise power of an initial laser input (a), where the noise characteristics at Ω approximate that of a coherent state $|\alpha\rangle$ and so quantum noise dominates the variance of intensity. The light is subsequently squeezed in amplitude (b) and then modulated in amplitude (c). The insets illustrate the ideal evolution of the state at $\pm\Omega$ for an initial coherent state $|\alpha\rangle$. The final state is amplitude squeezed with an average photon number of $\langle \hat{n}(\pm\Omega) \rangle = \delta_m |\alpha|^2 / 2$.

We derive an estimator for δ_m from the SNR of direct photodetection, similar to [18] which uses homodyne detection. For direct photodetection of AM in a shot-noise limited bandwidth around Ω , the SNR is given by $\delta_{SNR} = \langle p_s \rangle / \langle p_n \rangle$, where $\langle p_s \rangle$ is the average signal component of the generated electronic power at Ω , and $\langle p_n \rangle$ is the average electronic power generated from optical noise. In the limit of weak AM ($\delta_m \ll 1$) our estimator is unbiased, and loss due to AM has a negligible effect on the squeezing parameter Φ and the average optical power on the modulator output. Therefore, average measured photocurrent is expressed as $i_0 = q\eta P(1 - (\delta_m/2))/\hbar\omega \approx q\eta P/\hbar\omega$, with electron charge q , photodiode efficiency η , reduced Planck constant

\hbar and carrier angular frequency ω . We then obtain

$$\delta_{SNR} = \frac{\langle p_s \rangle}{\langle p_n \rangle} \approx \frac{\delta_m^2 i_0}{4q\Phi B}, \quad (1)$$

(see Appendix Section 1), where B is the frequency resolution bandwidth (RBW) of the noise spectrum, and corresponds to the inverse of the integration time over which the spectrum is measured. From equation (1), we define the estimator

$$\hat{\delta}_m = \sqrt{4\Phi B \chi^{-1} \hat{\delta}_{SNR}}, \quad (2)$$

where

$$\hat{\delta}_{SNR} = (p_\Omega - p_N)(p_N - p_E)^{-1}, \quad \text{and} \quad \chi = \eta \langle P \rangle (\hbar\omega)^{-1}. \quad (3)$$

p_Ω , p_N and p_E are the measured spectral noise powers of the electronic sideband, the optical noise floor and the electronic noise floor respectively. $\langle P \rangle$ is the average optical power output from the modulator, and both $\langle P \rangle$ and p_N may be pre-calibrated with high precision. The dependence of $\hat{\delta}_m$ on the optical noise is then contained in the measurement of p_Ω .

For an input resistance of R to the measuring device (e.g. spectrum analyser or oscilloscope), we can define the power of the electronic sideband as

$$p_\Omega = 2R \int_{\Omega - \frac{B}{2}}^{\Omega + \frac{B}{2}} |\hat{i}(\nu)|^2 d\nu, \quad (4)$$

where $|\hat{i}(\nu)|^2$ is the power spectral density of the measured current. By considering power fluctuations due to quantum

optical noise, low frequency classical optical noise, and electronic noise, we find

$$\text{Var}(p_\Omega) = \langle p_\Omega^2 \rangle - \langle p_\Omega \rangle^2 \approx R^2 \left[2\Phi q \delta_1^2 i_0^3 [\text{Cov}(\mathcal{H}_0, \mathcal{H})B + 1] + \frac{\delta_1^4 i_0^4}{4} \text{Var}(\mathcal{H}_0) + 4q^4 \text{Var}(\mathcal{N}) \right] \quad (5)$$

(see Appendix Section 2). $\text{Cov}(\bullet)$ is the covariance, \mathcal{H} is the total fractional classical intensity noise from the laser and modulator, \mathcal{H}_0 is the DC component of this classical noise, and \mathcal{N} is the electronic noise current in the $\pm B$ frequency interval around Ω . The dependence of $\text{Var}(p_\Omega)$ on \mathcal{H}_0 is due to classical noise being transferred from the carrier to the optical sidebands upon modulation. We assume here that the variance of the optical noise due to the classical intensity fluctuations scales quadratically with optical power, as expected for technical laser noise [25]. To quantify any advantage in precision obtained by using squeezed light, we compute the classical Fisher information on δ_m , $\mathcal{F}(\delta_m)$. Since we use an amplitude squeezed state to perform an amplitude measurement, the classical Fisher information saturates the quantum Cramér-Rao bound [26] — therefore evaluating $\mathcal{F}(\delta_m)$ bounds any quantum strategy. For our measurement strategy, and assuming $\alpha \gg 1$, δ_{SNR} is normally distributed and we can define $\mathcal{F}(\delta_{SNR})$ according to [27]

$$\mathcal{F}(\delta_{SNR}) = \frac{1}{\text{Var}(\delta_{SNR})} = \left[\left(\frac{\partial \delta_{SNR}}{\partial p_\Omega} \right)^2 \text{Var}(p_\Omega) \right]^{-1}. \quad (6)$$

$\mathcal{F}(\delta_m)$ can be obtained from $\mathcal{F}(\delta_{SNR})$ by using [27]

$$\mathcal{F}(\delta_m) = \left(\frac{\partial \delta_{SNR}}{\partial \delta_m} \right)^2 \mathcal{F}(\delta_{SNR}). \quad (7)$$

We find that when the power in the electronic sideband is much greater than the power in the electronic noise, $\text{Var}(\mathcal{N})$ contributes negligibly to $\mathcal{F}(\delta_m)$, and from equation (2-7), this leads to

$$\mathcal{F}(\delta_m) \approx \left[2\Phi \left(\frac{\text{Cov}(\mathcal{H}_0, \mathcal{H})B + 1}{\chi} \right) + \frac{\delta_m^2 \text{Var}(\mathcal{H}_0)}{4} \right]^{-1} \quad (8)$$

The quantum advantage is then the ratio $\mathcal{Q}(\delta_m)$ between the values of $\mathcal{F}(\delta_m)$ for a squeezed ($\Phi < 1$) and coherent ($\Phi = 1$) state. In the case that $\text{Cov}(\mathcal{H}_0, \mathcal{H}) \approx \text{Var}(\mathcal{H}_0)$ (e.g. weak spectral correlations in classical noise, or large DC classical noise), the quantum advantage becomes independent of the DC classical noise level in the limit $\text{Var}(\mathcal{H}_0)B \gg 1$.

Fig. 1(d) illustrates the dependence of $\mathcal{F}(\delta_m)$ on the RBW for a coherent state (solid black line) and various levels of squeezing (dashed lines), with all other parameters fixed. We see a reduction in $\mathcal{F}(\delta_m)$ as the RBW increases, since the quantum noise term scales linearly with B . We also find that for higher RBWs, squeezing provides sub-QNL precision in

estimating δ_m . This can be seen from equation (8), since for $2\Phi B/\chi \gg \delta_m^2/4$, we find $\mathcal{Q}(\delta_m) \rightarrow \mathcal{Q}_{opt}$, where

$$\mathcal{Q}_{opt} = 1/\Phi. \quad (9)$$

Because all information on δ_m is contained at modulation frequency Ω , this model suggests a practically achievable quantum advantage per photon in the probe. The requirement of higher RBWs to achieve a quantum advantage in precision means that our approach is applicable to experiments where there is a restriction in the maximum measurement duration, for example in the case that the sample is dynamically changing with time, or where the sample may only be exposed to a limited total photon dose. Due to the dependence of equation (8) on the classical noise, the quantum advantage described corresponds only to a reduction below the QNL, and not below the SQL. However, for systems with low classical noise ($\text{Var}(\mathcal{H}_0)B \ll 1$), equation (8) gives $\mathcal{F}(\delta_m) \approx 2\Phi/\chi$, which suggests that in this case a sub-SQL measurement may be achieved.

For the measurement, we built a source of amplitude squeezed light, based on [28]. 100 fs pulses with central wavelength $\lambda_0 = 740$ nm from a Ti:Sapphire laser are coupled into an asymmetric Sagnac interferometer, with a 90:10 splitting ratio beamsplitter (BS) (fig. 1(e)). 14 m of photonic crystal fibre (PCF) provides a strong $\chi^{(3)}$ nonlinearity in the interferometer. The fibre samples used were originally fabricated for photon pair generation work [29]. As the brighter 90% reflected pulses propagate through the PCF, they undergo self-phase modulation and become quadrature squeezed [10, 28]. These pulses interfere with the weaker (10%) counter-propagating pulses transmitted initially at the BS — these provide a coherent displacement in phase space. This leads to amplitude squeezing on the output of the interferometer [10]. The average optical power of the output state is 0.2 mW, which equates to 25 W of peak power. The amplitude squeezed light passes through an electro-optic modulator (EOM), that modulates polarisation. A subsequent polarising beamsplitter (PBS) translates the polarisation modulation into a weak AM of depth δ_m , and generates optical sidebands at distance $\pm\Omega$ from the carrier frequency. The resulting state is measured with direct detection, by collecting all the light at photodiode PD1. We calibrate the shot-noise level using the balanced subtraction photocurrent of PD1 and PD2.

Fig. 2(a) shows the relative noise power traces of amplitude modulated squeezed light (−1.2 dB) and antisqueezed light (2.7 dB) produced by the setup, accounting for electronic noise. The RBW is $B = 10$ kHz, which is considerably wider than the linewidth of the optical sidebands, measured to be ~ 1 Hz. The frequency separation of trace points in fig. 2(a) is smaller than the RBW due to the sampling rate of the SA being higher than the RBW. This measurement demonstrates enhanced sensitivity detection of AM due to amplitude squeezing, as already shown in [18].

Due to the Cramér-Rao bound [27], we know from equation (8) that the bound on $\text{Var}(\delta_m)$ is proportional to Φ and inversely proportional to $\langle P \rangle$. However, the profile of squeezing

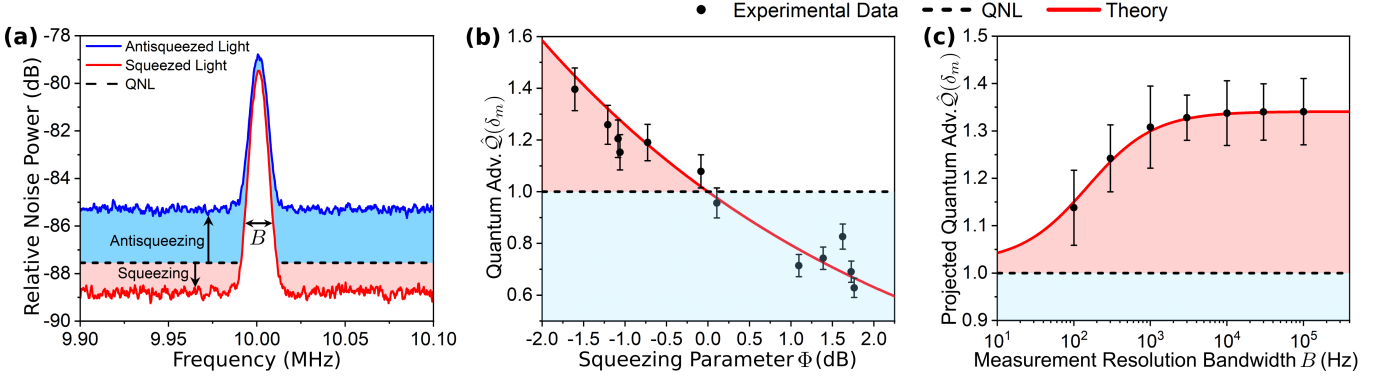


Figure 2. Observing a quantum advantage in parameter estimation using amplitude squeezed light. (a) 10 MHz AM measured by direct detection. The red trace corresponds to -1.2 dB of squeezing, and the blue trace to 2.7 dB of antisqueezing. The black dashed line marks the QNL. (b) Measured quantum advantage in precision of experimentally estimated δ_m , $\hat{Q}(\delta_m)$, for different squeezing Φ . The red line corresponds to Q_{opt} . (c) Measured $\hat{Q}(\delta_m)$ with varied RBWs B , for an average -1.3 dB of squeezing. See Methods for error bars.

with optical power is such that change in power is negligible across the maximum observed squeezing range $[-1.6, 2.7]$ dB in our setup, so here $\text{Var}(\delta_m)$ scales approximately linearly with Φ . By fitting measured $\text{Var}(\delta_m)$ to a line, we infer measured quantum advantage using

$$\hat{Q}(\delta_m) = \frac{\text{Var}(\delta_m)_{SN}}{\text{Var}(\delta_m)_{\Phi}}, \quad (10)$$

where $\text{Var}(\delta_m)_{SN}$ and $\text{Var}(\delta_m)_{\Phi}$ are variances of estimates of δ_m , for coherent and squeezed light respectively.

Fig. 2(b) shows measured $\hat{Q}(\delta_m)$ for a range of squeezing Φ with fixed RBW $B = 100$ kHz. The value of δ_m had a small experimental drift which varied between $\delta_m = [1.1, 1.3] \times 10^{-4}$ over the duration of the measurements. The RBW used means quantum noise limits the variance of δ_m , and the measurement saturates the optimal quantum bound Q_{opt} given by equation (9) (red curve). A quantum advantage of $\hat{Q}(\delta_m) = 1.40 \pm 0.08$ is observed with -1.6 dB of squeezing, in agreement with equation (9), since $\hat{Q}(\delta_m) \approx Q_{opt} = 1.44$. By repeating this for a range of B and a fixed -1.3 dB of average squeezing, we plot in fig. 2(c) the dependence of $\hat{Q}(\delta_m)$ on RBW. The red curve is a theoretical fitting calculated using equation (8), with $\text{Var}(\mathcal{H})$ and $\text{Cov}(\mathcal{H}_0, \mathcal{H})$ as fitting parameters. We observe sub-QNL precision down to $B = 100$ Hz. The maximum quantum advantage observed here is $\hat{Q}(\delta_m) = 1.34 \pm 0.07$, which again closely agrees with the the optimal $Q_{opt} = 1.35$ for the average squeezing parameter of $\Phi = 0.74$. Reducing optical loss to measure higher squeezing [9] enables greater enhancement in precision. Accounting for detection efficiency (we measure $\eta_d = 0.84$) and coupling efficiency between the interferometer output and the detector ($\eta_{opt} = 0.81$), we infer our maximum measured squeezing value of -1.6 dB corresponds to -2.6 dB of generated amplitude squeezing.

We have demonstrated quantum enhanced precision parameter estimation with bright squeezed amplitude light. Our model and experiment shows the degree of precision

is dictated by the amount of squeezing, the RBW and the classical noise on the generated sidebands. This exemplifies that for measurements of high power optical signals, sub-shot-noise sensitivity does not alone imply sub-shot-noise precision. However, squeezed light sub-shot-noise sensitivity spectroscopy and microscopy demonstrations have used kHz–MHz RBWs [30, 31], indicating possible sub-QNL precision in such applications using our work. We also motivate the possibility of achieving high power quantum precision improvement beyond the SQL for systems with low DC classical noise. We verify our model with experiment, reporting up to a 40% quantum advantage in precision in the estimation of the modulation index, per photon in the probe. We achieve this by using amplitude squeezed light of 0.2 mW average optical power (25 W peak power) as a probe, while our model shows a greater advantage is attainable with higher squeezing levels [24]. This power is comparable to the photon dose required to induce a photophobic response in living cells [32], therefore indicating this technique’s relevance to biological measurements.

* george.atkinson@bristol.ac.uk

† euan.allen@bristol.ac.uk

‡ jonathan.matthews@bristol.ac.uk

- [1] H. A. Bachor and T. C. Ralph. *A Guide to Experiments in Quantum Optics*, volume 1. Wiley Online Library, 2004.
- [2] B. L. Higgins, D. W. Berry, S. D. Bartlett, H. M Wiseman, and G. J Pryde. Entanglement-free heisenberg-limited phase estimation. *Nat.*, 450:393–396, 2007.
- [3] P. M. Birchall, J. L. O’Brien, J. C. F. Matthews, and H. Cable. Quantum-classical boundary for precision optical phase estimation. *Phys. Rev. A*, 96(6):062109, 2017.
- [4] E. J. Allen et al. Approaching the quantum limit of precision in absorbance estimation using classical resources. *Phys. Rev. Research*, 2:033243, 2020.
- [5] R. Cole. Live-cell imaging: The cell’s perspective. *Cell Adh Migr*, 8(5):452–459, 2014.
- [6] M. Xiao, L.-A. Wu, and H. J. Kimble. Precision measurement beyond the shot-noise limit. *Phys. Rev. Lett.*, 59(3):278, 1987.

- [7] M. A. Taylor et al. Biological measurement beyond the quantum limit. *Nat. Photonics*, 7(3):229, 2013.
- [8] C. Gardiner and P. Zoller. *Quantum Noise: A Handbook of Markovian and Non-Markovian Quantum Stochastic Methods with Applications to Quantum Optics*, volume 56. Springer Science & Business Media, 2004.
- [9] H. Vahlbruch, M. Mehmet, K. Danzmann, and R. Schnabel. Detection of 15 db squeezed states of light and their application for the absolute calibration of photoelectric quantum efficiency. *Phys. Rev. Lett.*, 117(11):110801, 2016.
- [10] U. L. Andersen, T. Gehring, C. Marquardt, and G. Leuchs. 30 years of squeezed light generation. *Phys. Scr.*, 91(5):053001, 2016.
- [11] M. Zwiernik, C. A. Pérez-Delgado, and P. Kok. General optimality of the heisenberg limit for quantum metrology. *Phys. Rev. Lett.*, 105(18):180402, 2010.
- [12] J. Minkoff. *Signal Processing Fundamentals and Applications for Communications and Sensing Systems*. Artech House, 2002.
- [13] S. Slussarenko et al. Unconditional violation of the shot-noise limit in photonic quantum metrology. *Nat. Photonics*, 11(11):700, 2017.
- [14] J. Sabines-Chesterking et al. Sub-shot-noise transmission measurement enabled by active feed-forward of heralded single photons. *Phys. Rev. Appl.*, 8(1):014016, 2017.
- [15] G. Brida, M. Genovese, and I. Rou Berchera. Experimental realization of sub-shot-noise quantum imaging. *Nat. Photonics*, 4:227, 2010.
- [16] A. A. Berni et al. Ab initio quantum-enhanced optical phase estimation using real-time feedback control. *Nat. Photonics*, 9(9):577, 2015.
- [17] H. Yonezawa et al. Quantum-enhanced optical-phase tracking. *Science*, 337(6101):1514–1517, 2012.
- [18] M. Xiao, L.-A. Wu, and H. J. Kimble. Detection of amplitude modulation with squeezed light for sensitivity beyond the shot-noise limit. *Opt. Lett.*, 13(6):476–478, 1988.
- [19] E. S. Polzik, J. Carri, and H. J. Kimble. Spectroscopy with squeezed light. *Phys. Rev. Lett.*, 68(20):3020, 1992.
- [20] M. Tse et al. Quantum-enhanced advanced ligo detectors in the era of gravitational-wave astronomy. *Phys. Rev. Lett.*, 123:231107, 2019.
- [21] F. Acernese et al. Increasing the astrophysical reach of the advanced virgo detector via the application of squeezed vacuum states of light. *Phys. Rev. Lett.*, 123:231108, 2019.
- [22] F. Wolfgramm et al. Squeezed-light optical magnetometry. *Phys. Rev. Lett.*, 105(5):053601, 2010.
- [23] C. A. Casacio et al. Quantum correlations overcome the photodamage limits of light microscopy. *Preprint at arXiv:2004.00178*, 2020.
- [24] D. Krylov and K. Bergman. Amplitude-squeezed solitons from an asymmetric fiber interferometer. *Opt. Lett.*, 23(17):1390–1392, 1998.
- [25] O. Svelto and D. C. Hanna. *Principles of Lasers*, volume 1. Springer, 2010.
- [26] O. Pinel, P. Jian, N. Treps, C. Fabre, and D. Braun. Quantum parameter estimation using general single-mode gaussian states. *Phys. Rev. A*, 88(4):040102, 2013.
- [27] E. L. Lehmann and G. Casella. *Theory of Point Estimation*. Springer Science & Business Media, 2006.
- [28] S. Schmitt et al. Photon-number squeezed solitons from an asymmetric fiber-optic sagnac interferometer. *Phys. Rev. Lett.*, 81(12):2446, 1998.
- [29] O. Alibart et al. Photon pair generation using four-wave mixing in a microstructured fibre: theory versus experiment. *New J. Phys.*, 8(5):67, 2006.
- [30] G. T. Garces et al. Quantum-enhanced stimulated emission detection for label-free microscopy. *Applied Physics Letters*, 117(2):024002, 2020.
- [31] F. Marin, A. Bramati, V. Jost, and E. Giacobino. Demonstration of high sensitivity spectroscopy with squeezed semiconductor lasers. *Opt. Commun.*, 140(1-3):146–157, 1997.
- [32] P. Berthold et al. Channelrhodopsin-1 initiates phototaxis and photophobic responses in chlamydomonas by immediate light-induced depolarization. *The Plant Cell*, 20(6):1665–1677, 2008.
- [33] R. Loudon. *The quantum theory of light*. OUP Oxford, 2000.
- [34] F. Quinlan, T. M Fortier, H. Jiang, and S. A Diddams. Analysis of shot noise in the detection of ultrashort optical pulse trains. *JOSA B*, 30(6):1775–1785, 2013.

Methods

The Ti:Sapphire laser is a Spectra Physics Mai Tai oscillator, configured to emit at one central wavelength $\lambda_0 = 740$ nm. The electro-optic modulator (EOM) is a Thorlabs EO-AM-NR-C1. The balanced amplified photodetector is a Thorlabs PDB440A(-AC) and the spectrum analyser (SA) is a Rohde & Schwarz FPC1000.

The chosen central wavelength of $\lambda_0 = 740$ nm is close to the 730 nm zero-dispersion wavelength of the PCF, in order to minimise the spectral broadening, which enables optimal interference at the 90:10 BS. The group velocity dispersion at λ_0 is $\beta = -2.06$ ps²/km. The zero-dispersion wavelength of the PCF may be tailored by the fibre structure, making this approach applicable to a large range of wavelengths. The PCF has an estimated core diameter of $2.09 \mu\text{m}$, with an attenuation coefficient of $\alpha_{dB} = 0.1$ dB/m. The high confinement of the light in the small core size of the PCF provides the strong $\chi^{(3)}$ nonlinearity for quadrature squeezing, relative to standard single-mode fibre.

The antisqueezed data in fig. 2(a) is corrected for the difference in optical power required to generate antisqueezing and squeezing, by subtracting the difference in the respective shot-noise levels from this trace. The electronic noise has also been subtracted from each trace. Each measurement of $\text{Var}(\delta_m)_\Phi$ is taken from 50 samples of δ_m . In fig. 2(b), the error bars indicate the standard deviations over 236 variance measurements. In fig. 2(c), the error bars were derived from the standard deviations over 10 evaluations of the quantum advantage from separate fittings to the data, where each fitting curve was based on an average of 23 variance measurements for each Φ .

Supporting data is available on request.

Acknowledgements

We thank J. Mueller, P. Mosley, A. Politi, J. Rarity, N. Samantaray, W. Wadsworth and S. Wollmann for helpful discussions. This work was supported by QuantIC - The UK Quantum Technology Hub in Quantum Imaging (EPSRC EP/T00097X/1). G.S.A. was supported by the Quantum Engineering Centre for Doctoral Training (EP-SRC EP/L015730/1). E.J.A. acknowledges fellowship support from EPSRC Doctoral Prize Fellowship (EP/R513179/1). J.C.F.M. acknowledges support from an EPSRC Quantum Technology Fellowship (EP/M024385/1) and European Research Council starting grant ERC-2018-STG 803665.

**APPENDIX:
QUANTUM ENHANCED PRECISION ESTIMATION WITH BRIGHT SQUEEZED LIGHT**

1. Calculation of the Signal-to-Noise Ratio

Here we derive the expected value of the electronic power p_Ω in the $\pm B/2$ frequency interval around the modulation frequency Ω , generated by the current $\hat{i}(t)$. We first define simplified notation for the limits of integration:

$$\int_{-B/2}^{B/2} \equiv \int^0, \quad \int_{\Omega-B/2}^{\Omega+B/2} \equiv \int^\Omega \quad \text{and} \quad \int_{-\infty}^{\infty} \equiv \int. \quad (11)$$

We may then write p_Ω as [1]

$$p_\Omega = 2R \int^\Omega S(\nu) d\nu, \quad (12)$$

where R is the input resistance, $S(\nu) = |\hat{i}(\nu)|^2$ is the power spectral density of the measured current at frequency ν , and the factor of 2 comes from the integration over positive and negative frequencies. The amplitude of the optical field $\hat{A}(t)$ may be written in terms of a classical field amplitude $\alpha(t)$ and the quantum component $\hat{a}(t)$, where $\alpha(t) = |\alpha(t)|e^{i\theta}$ and θ is the phase of the classical field. The current at time t may then be written as

$$\hat{i}(t) = q \left(\hat{A}(t)^\dagger \hat{A}(t) + n_e(t) \right) = q \left(|\alpha(t)|^2 + \sqrt{2}|\alpha(t)|\hat{x}_\theta(t) + \hat{a}(t)^\dagger \hat{a}(t) + n_e(t) \right), \quad (13)$$

where we have defined the quadrature amplitude operator $\hat{x}_\theta(t) = \frac{1}{\sqrt{2}}[\hat{a}(t)e^{-i\theta} + \hat{a}(t)^\dagger e^{i\theta}]$ and $n_e(t)$ corresponds to the number of electrons generated independently of the optical field. Here we model the detection efficiency η as an additional loss before detection, and η is therefore incorporated into $\alpha(t)$. The component of the photocurrent at frequency ν may then be written as

$$\hat{i}(\nu) = q \left[I(\nu) + \sqrt{2} \int \alpha(\bar{\nu}) \hat{x}_\theta(\nu - \bar{\nu}) d\bar{\nu} + \int \hat{a}(-\bar{\nu})^\dagger \hat{a}(\nu - \bar{\nu}) d\bar{\nu} \right], \quad (14)$$

where we define the unitary Fourier transforms

$$I(\nu) = \int (|\alpha(t)|^2 + n_e(t)) e^{-2\pi i \nu t} dt \quad (15)$$

and

$$\hat{x}(\nu) = \int \hat{x}_\theta(t) e^{-2\pi i \nu t} dt = \hat{a}(-\nu)^\dagger e^{i\theta} + \hat{a}(\nu) e^{-i\theta}. \quad (16)$$

We also define $\hat{a}(\nu)$ as the squeezed vacuum operator [33]

$$\hat{a}(\nu) = \hat{b}(\nu) \cosh r(\nu) - e^{2i\theta(\nu)} \hat{b}(-\nu)^\dagger \sinh r(\nu), \quad (17)$$

where $\hat{b}(\nu)$ and $\hat{b}(\nu)^\dagger$ are the bosonic creation and annihilation operators. The squeezing is defined such that $r(\nu) = r$ and $\theta(\nu) = \theta$ within the frequency bandwidth $-\Lambda/2 \leq \nu \leq \Lambda/2$ (where $\Lambda/2 > \Omega$) and $r(\nu) = 0$ outside of this frequency range. The 2θ phase factor therefore orients the squeezing in the amplitude direction. We can then write the power spectral density as

$$\begin{aligned} S(\nu) = q^2 \bigg[& |I(\nu)|^2 + \sqrt{2} I(\nu)^* \int \alpha(\bar{\nu}) \hat{x}_\theta(\nu - \bar{\nu}) d\bar{\nu} + I(\nu)^* \int \hat{a}(-\bar{\nu})^\dagger \hat{a}(\nu - \bar{\nu}) d\bar{\nu} \\ & \sqrt{2} I(\nu) \int \alpha(\bar{\nu})^* \hat{x}_\theta(\nu - \bar{\nu})^\dagger d\bar{\nu} + 2 \iint \alpha(\bar{\nu})^* \alpha(\bar{\bar{\nu}}) \hat{x}_\theta(\nu - \bar{\nu})^\dagger \hat{x}_\theta(\nu - \bar{\bar{\nu}}) d\bar{\nu} d\bar{\bar{\nu}} \\ & + \sqrt{2} \iint \alpha(\bar{\nu})^* \hat{x}_\theta(\nu - \bar{\nu})^\dagger \hat{a}(-\bar{\bar{\nu}})^\dagger \hat{a}(\nu - \bar{\bar{\nu}}) d\bar{\nu} d\bar{\bar{\nu}} + I(\nu) \int \hat{a}(\nu - \bar{\nu})^\dagger \hat{a}(-\bar{\nu}) d\bar{\nu} \\ & + \sqrt{2} \iint \alpha(\bar{\bar{\nu}}) \hat{a}(\nu - \bar{\nu})^\dagger \hat{a}(-\bar{\nu}) \hat{x}_\theta(\nu - \bar{\bar{\nu}}) d\bar{\nu} d\bar{\bar{\nu}} + \iint \hat{a}(\nu - \bar{\nu})^\dagger \hat{a}(-\bar{\nu}) \hat{a}(-\bar{\bar{\nu}})^\dagger \hat{a}(\nu - \bar{\bar{\nu}}) d\bar{\nu} d\bar{\bar{\nu}} \bigg], \quad (18) \end{aligned}$$

where $(\bullet)^*$ denotes the complex conjugate. The magnitude of the classical field amplitude $|\alpha(t)|$ can be written in terms of the mean value of the amplitude before modulation, α_0 , and the time dependent components as

$$|\alpha(t)| = \sqrt{\eta}\alpha_0 [\Psi_0 + \Psi_m \cos(2\pi\Omega t) + \zeta(t)], \quad (19)$$

where we have assumed a continuous-wave amplitude for simplicity, and $\zeta(t)$ is a stochastic classical noise function that describes the combined effect of classical laser noise and modulator noise on the optical field. In terms of the modulation index δ_m , $\Psi_0 = 1 - \delta_m/2$ and $\Psi_m = \delta_m/2$. We can then find the frequency dependence of the classical field amplitude:

$$\alpha(\nu) = \alpha \left[\Psi_0 \delta(\nu) + \frac{\Psi_m}{2} (\delta(\Omega - \nu) + \delta(\Omega + \nu)) + h(\nu) \right], \quad (20)$$

where $\alpha = \sqrt{\eta}\alpha_0$, $h(\nu) = \int \zeta(t) e^{-2\pi i \nu t} dt$, and since classical noise is only observed at low frequencies ($\lesssim 2\text{MHz}$), we can write for example $h(\Omega) = 0$. Also, the zero frequency components of both $h(0) = \int \zeta(t) dt$ and $n_e(0) = \int n_e(t) dt$ vanish since this corresponds to the average in the limit of infinite time. Equation (19) allows us to define $I(\nu)$ as

$$I(\nu) = \alpha^2 \left[\Psi_0^2 \delta(\nu) + \Psi_0 \Psi_m [\delta(\Omega - \nu) + \delta(\Omega + \nu)] + 2\Psi_0 h(\nu) + \int h(\bar{\nu}) h(\nu - \bar{\nu}) d\bar{\nu} \right. \\ \left. + \frac{\Psi_m^2}{4} [\delta(2\Omega - \nu) + \delta(2\Omega + \nu) + 2\delta(\nu)] + \Psi_m [h(\nu - \Omega) + h(\nu + \Omega)] \right] + n_e(\nu). \quad (21)$$

We can then find the expectation $\langle p_\Omega \rangle$ with respect to the random variables $h(\nu)$, $n_e(\nu)$ and $\hat{x}(\nu)$. Since these variables are independent, the expectation value may be defined as $\langle \bullet \rangle \equiv \langle \langle 0 | \bullet | 0 \rangle \rangle_{h(\nu)} n_e(\nu)$. To calculate this, we can first compute

$$\int^\Omega |I(\nu)|^2 d\nu = \Psi_0^2 \Psi_m^2 \alpha^4 + 2\Psi_0 \Psi_m \alpha^2 \Re[n_e(\Omega)] \\ + \Psi_m^2 \alpha^4 \int^0 |h(\nu)|^2 d\nu + 2\Psi_m \alpha^2 \int^\Omega \Re[h(\nu - \Omega)^* n_e(\nu)] d\nu + \int^\Omega |n_e(\nu)|^2 d\nu, \quad (22)$$

where $\Re[\bullet]$ signifies the real part. Then, by evaluating the quantum part of the expectation value, we obtain the result

$$\langle p_\Omega \rangle = 2R \int^\Omega \langle S(\nu) \rangle d\nu = 2q^2 R \left[\int^\Omega \langle |I(\nu)|^2 \rangle d\nu + \Phi \int^\Omega \int^\Omega \langle |\alpha(\bar{\nu})|^2 \rangle d\bar{\nu} d\nu + B\Lambda \left(\frac{\Phi^2}{8} + \frac{1}{8\Phi^2} - \frac{1}{4} \right) \right] \\ = 2q^2 R \left[\alpha^4 \left(\Psi_0^2 \Psi_m^2 + \Psi_m^2 \int^0 \langle |h(\nu)|^2 \rangle d\nu \right) + \int^\Omega \langle |n_e(\nu)|^2 \rangle d\nu + B\Lambda \left(\frac{\Phi^2}{8} + \frac{1}{8\Phi^2} - \frac{1}{4} \right) \right. \\ \left. + \alpha^2 \left(\Psi_0^2 \Phi B + \frac{\Psi_m^2 \Phi B}{2} + \Phi B \int^\Omega \langle |h(\nu)|^2 \rangle d\nu + 2\Psi_0 \Psi_m \langle \Re[n_e(\Omega)] \rangle + 2\Psi_m \int^\Omega \langle \Re[h(\nu - \Omega)^* n_e(\nu)] \rangle d\nu \right) \right], \quad (23)$$

for the squeezing parameter $\Phi = e^{-2r}$. In equation (23), we have neglected terms involving the expectation value of the product of an odd number of creation or annihilation operators, and terms outside the domain of $h(\nu)$. By observing that $\int \langle |h(\nu)|^2 \rangle d\nu \ll 1$ and $\delta_m \ll 1$, and associating $i_0 \approx q\alpha^2$ we find

$$\langle p_\Omega \rangle \approx R \left(\frac{i_0^2 \delta_m^2}{2} + 2qi_0 \Phi B + 2q^2 \int^\Omega \langle |n_e(\nu)|^2 \rangle d\nu \right). \quad (24)$$

Similarly, at a small frequency interval Δf from Ω , we find that the electronic power of the optical noise floor and electronic noise floor are respectively

$$\langle p_N \rangle \approx R \left(2qi_0 \Phi B + 2q^2 \int^\Omega \langle |n_e(\nu)|^2 \rangle d\nu \right) \quad \text{and} \quad \langle p_E \rangle = R \left(2q^2 \int^\Omega \langle |n_e(\nu)|^2 \rangle d\nu \right). \quad (25)$$

We then find that the optical signal-to-noise ratio δ_{SNR} may be expressed as

$$\delta_{SNR} = \frac{\langle p_\Omega \rangle - \langle p_N \rangle}{\langle p_N \rangle - \langle p_E \rangle} \approx \frac{i_0 \delta_m^2}{4q\Phi B}. \quad (26)$$

2. Calculation of the Variance of the Sideband Power

In order to calculate the variance $\text{Var}(p_\Omega) = \langle p_\Omega^2 \rangle - \langle p_\Omega \rangle^2$, an expression for $\langle p_\Omega \rangle^2$ may be evaluated directly from equation (23) to give

$$\begin{aligned}
\langle p_\Omega \rangle^2 = & 4q^4 R^2 \left[\alpha^8 \left[\Psi_0^4 \Psi_m^4 + 2\Psi_0^2 \Psi_m^4 \int^0 \langle |h(\nu)|^2 \rangle d\nu + \Psi_m^4 \int^0 \int^0 \langle |h(\nu)|^2 \rangle \langle |h(\bar{\nu})|^2 \rangle d\nu d\bar{\nu} \right] \right. \\
& + \alpha^6 \left[4\Psi_0^3 \Psi_m^3 \langle \Re[n_e(\Omega)] \rangle + 4\Psi_0^2 \Psi_m^3 \int^\Omega \langle \Re[h(\nu - \Omega)^* n_e(\nu)] \rangle d\nu + 2\Phi B \Psi_0^4 \Psi_m^2 + \Phi B \Psi_0^2 \Psi_m^4 \right. \\
& \quad + 2\Phi B \Psi_0^2 \Psi_m^2 \int \langle |h(\nu)|^2 \rangle d\nu + 4\Psi_0 \Psi_m^3 \langle \Re[n_e(\Omega)] \rangle \int^0 \langle |h(\nu)|^2 \rangle d\nu \\
& \quad + 4\Psi_m^3 \int^\Omega \int^0 \langle |h(\nu)|^2 \rangle \langle \Re[h(\bar{\nu} - \Omega)^* n_e(\bar{\nu})] \rangle d\nu d\bar{\nu} + 2\Phi B \Psi_0^2 \Psi_m^2 \int^0 \langle |h(\nu)|^2 \rangle d\nu + \Phi B \Psi_m^4 \int^0 \langle |h(\nu)|^2 \rangle d\nu \\
& \quad \left. + 2\Phi B \Psi_m^2 \int \int^0 \langle |h(\nu)|^2 \rangle \langle |h(\bar{\nu})|^2 \rangle d\nu d\bar{\nu} \right] + \alpha^4 \left[2\Psi_0^2 \Psi_m^2 \int^\Omega \langle |n_e(\nu)|^2 \rangle d\nu + \Psi_0^2 \Psi_m^2 B \Lambda \left(\frac{\Phi^2}{4} + \frac{1}{4\Phi^2} - \frac{1}{2} \right) \right. \\
& \quad + 4\Psi_0^2 \Psi_m^2 \langle \Re[n_e(\Omega)] \rangle^2 + 8\Psi_0 \Psi_m^2 \langle \Re[n_e(\Omega)] \rangle \int^\Omega \langle \Re[h(\nu - \Omega)^* n_e(\nu)] \rangle d\nu + 4\Phi B \Psi_0^3 \Psi_m \langle \Re[n_e(\Omega)] \rangle \\
& \quad + 2\Phi B \Psi_0 \Psi_m^3 \langle \Re[n_e(\Omega)] \rangle + 4\Phi B \Psi_0 \Psi_m \langle \Re[n_e(\Omega)] \rangle \int \langle |h(\nu)|^2 \rangle d\nu \\
& \quad + 2\Psi_m^2 \int^\Omega \int^0 \langle |h(\nu)|^2 \rangle \langle |n_e(\bar{\nu})|^2 \rangle d\nu d\bar{\nu} + \Psi_m^2 B \Lambda \left(\frac{\Phi^2}{4} + \frac{1}{4\Phi^2} - \frac{1}{2} \right) \int^0 \langle |h(\nu)|^2 \rangle d\nu \\
& \quad + 4\Psi_m^2 \int^\Omega \int^\Omega \langle \Re[h(\nu - \Omega)^* n_e(\nu)] \rangle \langle \Re[h(\bar{\nu} - \Omega)^* n_e(\bar{\nu})] \rangle d\nu d\bar{\nu} + 4\Phi B \Psi_0^2 \Psi_m \int^\Omega \langle \Re[h(\nu - \Omega)^* n_e(\nu)] \rangle d\nu \\
& \quad + 2\Phi B \Psi_m^3 \int^\Omega \langle \Re[h(\nu - \Omega)^* n_e(\nu)] \rangle d\nu + 4\Phi B \Psi_m \int \int^\Omega \langle \Re[h(\nu - \Omega)^* n_e(\nu)] \rangle \langle |h(\bar{\nu})|^2 \rangle d\nu d\bar{\nu} \\
& \quad + \Phi^2 B^2 \Psi_0^4 + \Phi^2 B^2 \Psi_0^2 \Psi_m^2 + 2\Phi^2 B^2 \Psi_0^2 \int \langle |h(\nu)|^2 \rangle d\nu + \frac{1}{4} \Phi^2 B^2 \Psi_m^4 + \Phi^2 B^2 \Psi_m^2 \int \langle |h(\nu)|^2 \rangle d\nu \\
& \quad + \Phi^2 B^2 \int \int \langle |h(\nu)|^2 \rangle \langle |h(\bar{\nu})|^2 \rangle d\nu d\bar{\nu} \left. \right] + \alpha^2 \left[4\Psi_0 \Psi_m \langle \Re[n_e(\Omega)] \rangle \int^\Omega \langle |n_e(\nu)|^2 \rangle d\nu \right. \\
& \quad + \Psi_0 \Psi_m \langle \Re[n_e(\Omega)] \rangle B \Lambda \left(\frac{\Phi^2}{2} + \frac{1}{2\Phi^2} - 1 \right) + 4\Psi_m \int^\Omega \int^\Omega \langle \Re[h(\nu - \Omega)^* n_e(\nu)] \rangle \langle |n_e(\bar{\nu})|^2 \rangle d\nu d\bar{\nu} \\
& \quad + \Psi_m B \Lambda \left(\frac{\Phi^2}{2} + \frac{1}{2\Phi^2} - 1 \right) \int^\Omega \langle \Re[h(\nu - \Omega)^* n_e(\nu)] \rangle d\nu + 2\Phi B \Psi_0^2 \int^\Omega \langle |n_e(\nu)|^2 \rangle d\nu \\
& \quad + \Phi B \Psi_m^2 \int^\Omega \langle |n_e(\nu)|^2 \rangle d\nu + 2\Phi B \int \int^\Omega \langle |n_e(\nu)|^2 \rangle \langle |h(\bar{\nu})|^2 \rangle d\nu d\bar{\nu} + \Phi B^2 \Psi_0^2 \Lambda \left(\frac{\Phi^2}{4} + \frac{1}{4\Phi^2} - \frac{1}{2} \right) \\
& \quad + \Phi B^2 \Psi_m^2 \Lambda \left(\frac{\Phi^2}{8} + \frac{1}{8\Phi^2} - \frac{1}{4} \right) + \Phi B^2 \Lambda \left(\frac{\Phi^2}{4} + \frac{1}{4\Phi^2} - \frac{1}{2} \right) \int \langle |h(\nu)|^2 \rangle d\nu \left. \right] \\
& \quad + \int^\Omega \int^\Omega \langle |n_e(\nu)|^2 \rangle \langle |n_e(\bar{\nu})|^2 \rangle d\nu d\bar{\nu} + B \Lambda \left(\frac{\Phi^2}{4} + \frac{1}{4\Phi^2} - \frac{1}{2} \right) \int^\Omega \langle |n_e(\nu)|^2 \rangle d\nu \\
& \quad \left. + B^2 \Lambda^2 \left(\frac{\Phi^4}{64} + \frac{1}{64\Phi^4} - \frac{\Phi^2}{16} - \frac{1}{16\Phi^2} + \frac{3}{32} \right) \right]. \quad (27)
\end{aligned}$$

To find an expression for $\langle p_\Omega^2 \rangle$, we can again neglect terms where the expectation value of the quadrature operators vanishes, giving

$$\begin{aligned}
\langle p_\Omega^2 \rangle = & 4q^4 R^2 \left\langle \int^\Omega \int^\Omega \left[|I(\nu)|^2 |I(\bar{\nu})|^2 + 4|I(\nu)|^2 \int \int \alpha(\bar{\nu})^* \alpha(\bar{\bar{\nu}}) \hat{x}_\theta(\bar{\nu} - \bar{\bar{\nu}})^\dagger \hat{x}_\theta(\bar{\nu} - \bar{\bar{\nu}}) d\bar{\bar{\nu}} d\bar{\bar{\bar{\nu}}} \right. \right. \\
& \left. \left. + 2I(\nu)^* I(\bar{\nu})^* \int \int \alpha(\bar{\nu}) \alpha(\bar{\bar{\nu}}) \hat{x}_\theta(\nu - \bar{\bar{\nu}}) \hat{x}_\theta(\bar{\nu} - \bar{\bar{\bar{\nu}}}) d\bar{\bar{\nu}} d\bar{\bar{\bar{\nu}}} + 2I(\nu) I(\bar{\nu}) \int \int \alpha(\bar{\nu})^* \alpha(\bar{\bar{\nu}})^* \hat{x}_\theta(\nu - \bar{\bar{\nu}})^\dagger \hat{x}_\theta(\bar{\nu} - \bar{\bar{\bar{\nu}}})^\dagger d\bar{\bar{\nu}} d\bar{\bar{\bar{\nu}}} \right] \right\rangle
\end{aligned}$$

$$\begin{aligned}
& + 4\Psi_0^2\Psi_m^3\alpha^6 \int^\Omega \langle \Re[h(\nu - \Omega)^* n_e(\nu)] \rangle d\nu + 2\Psi_0^2\Psi_m^2\alpha^4 \int^\Omega \langle |n_e(\nu)|^2 \rangle d\nu + 4\Psi_0^2\Psi_m^2\alpha^4 \langle \Re[n_e(\Omega)]^2 \rangle \\
& + 4\Psi_0\Psi_m^3\alpha^6 \int^\Omega \langle \Re[n_e(\Omega)] |h(\nu)|^2 \rangle d\nu + 8\Psi_0\Psi_m^2\alpha^4 \int^\Omega \langle \Re[h(\nu - \Omega)^* n_e(\nu)] \Re[n_e(\Omega)] \rangle d\nu \\
& + 4\Psi_0\Psi_m\alpha^2 \int^\Omega \langle |n_e(\nu)|^2 \Re[n_e(\Omega)] \rangle d\nu + \Psi_m^4\alpha^8 \int^0 \int^0 \langle |h(\nu)|^2 |h(\bar{\nu})|^2 \rangle d\nu d\bar{\nu} \\
& + 4\Psi_m^3\alpha^6 \int^\Omega \int^0 \langle |h(\nu)|^2 \Re[h(\bar{\nu} - \Omega)^* n_e(\bar{\nu})] \rangle d\nu d\bar{\nu} + 2\Psi_m^2\alpha^4 \int^\Omega \int^0 \langle |h(\nu)|^2 |n_e(\bar{\nu})|^2 \rangle d\nu d\bar{\nu} \\
& + 4\Psi_m^2\alpha^4 \int^\Omega \int^\Omega \langle \Re[h(\nu - \Omega)^* n_e(\nu)] \Re[h(\bar{\nu} - \Omega)^* n_e(\bar{\nu})] \rangle d\nu d\bar{\nu} + 4\Psi_m\alpha^2 \int^\Omega \int^\Omega \langle \Re[h(\nu - \Omega)^* n_e(\nu)] |n_e(\bar{\nu})|^2 \rangle d\nu d\bar{\nu} \\
& + \int^\Omega \int^\Omega \langle |n_e(\nu)|^2 |n_e(\bar{\nu})|^2 \rangle d\nu d\bar{\nu}. \quad (29)
\end{aligned}$$

For term 2 of equation (28):

$$\begin{aligned}
& \left\langle 4 \int \int \int^\Omega \int^\Omega |I(\nu)|^2 \alpha(\bar{\nu})^* \alpha(\bar{\bar{\nu}}) \hat{x}_\theta(\bar{\nu} - \bar{\bar{\nu}})^\dagger \hat{x}_\theta(\bar{\nu} - \bar{\bar{\nu}}) d\nu d\bar{\nu} d\bar{\bar{\nu}} \right\rangle = 2\Phi \int \int^\Omega \int^\Omega \langle |I(\nu)|^2 |\alpha(\bar{\nu})|^2 \rangle d\nu d\bar{\nu} d\bar{\bar{\nu}} \\
& = 2\Phi B \Psi_0^4 \Psi_m^2 \alpha^6 + \Phi B \Psi_0^2 \Psi_m^4 \alpha^6 + 2\Phi B \Psi_0^2 \Psi_m^2 \alpha^6 \int \langle |h(\bar{\nu})|^2 \rangle d\bar{\nu} + 4\Phi B \Psi_0^3 \Psi_m \alpha^4 \langle \Re[n_e(\Omega)] \rangle + 2\Phi B \Psi_0 \Psi_m^3 \alpha^4 \langle \Re[n_e(\Omega)] \rangle \\
& + 4\Phi B \Psi_0 \Psi_m \alpha^4 \int \langle \Re[n_e(\Omega)] |h(\bar{\nu})|^2 \rangle d\bar{\nu} + 2\Phi B \Psi_0^2 \Psi_m^2 \alpha^6 \int^0 \langle |h(\nu)|^2 \rangle d\nu + \Phi B \Psi_m^4 \alpha^6 \int^0 \langle |h(\nu)|^2 \rangle d\nu \\
& + 2\Phi B \Psi_m^2 \alpha^6 \int \int^0 \langle |h(\nu)|^2 |h(\bar{\nu})|^2 \rangle d\nu d\bar{\nu} + 4\Phi B \Psi_0^2 \Psi_m \alpha^4 \int^\Omega \langle \Re[h(\nu - \Omega)^* n_e(\nu)] \rangle d\nu \\
& + 2\Phi B \Psi_m^3 \alpha^4 \int^\Omega \langle \Re[h(\nu - \Omega)^* n_e(\nu)] \rangle d\nu + 4\Phi B \Psi_m \alpha^4 \int \int^\Omega \langle \Re[h(\nu - \Omega)^* n_e(\nu)] |h(\bar{\nu})|^2 \rangle d\nu d\bar{\nu} \\
& + 2\Phi B \Psi_0^2 \alpha^2 \int^\Omega \langle |n_e(\nu)|^2 \rangle d\nu + \Phi B \Psi_m^2 \alpha^2 \int^\Omega \langle |n_e(\nu)|^2 \rangle d\nu + 2\Phi B \alpha^2 \int \int^\Omega \langle |n_e(\nu)|^2 |h(\bar{\nu})|^2 \rangle d\nu d\bar{\nu}. \quad (30)
\end{aligned}$$

Term 3 of equation (28) may be calculated by first evaluating the part which is dependent on ν and $\bar{\nu}$:

$$\begin{aligned}
& \left\langle 2 \int \int \alpha(\bar{\nu}) \alpha(\bar{\bar{\nu}}) \int^\Omega \int^\Omega I(\nu)^* I(\bar{\nu})^* \hat{x}_\theta(\nu - \bar{\nu}) \hat{x}_\theta(\bar{\nu} - \bar{\bar{\nu}}) d\nu d\bar{\nu} d\bar{\bar{\nu}} \right\rangle \\
& = \left\langle 2 \int \int \alpha(\bar{\nu}) \alpha(\bar{\bar{\nu}}) \left[\frac{\Phi}{2} \Psi_0^2 \Psi_m^2 \alpha^4 \delta(2\Omega - \bar{\nu} - \bar{\bar{\nu}}) + \Psi_0 \Psi_m^2 \alpha^4 \int^\Omega h(\bar{\nu} - \Omega)^* \langle 0 | \hat{x}_\theta(\Omega - \bar{\nu}) \hat{x}_\theta(\bar{\nu} - \bar{\bar{\nu}}) | 0 \rangle d\bar{\nu} \right. \right. \\
& + \Psi_0 \Psi_m \alpha^2 \int^\Omega n_e(\bar{\nu})^* \langle 0 | \hat{x}_\theta(\Omega - \bar{\nu}) \hat{x}_\theta(\bar{\nu} - \bar{\bar{\nu}}) | 0 \rangle d\bar{\nu} + \Psi_0 \Psi_m^2 \alpha^4 \int^\Omega h(\nu - \Omega)^* \langle 0 | \hat{x}_\theta(\nu - \bar{\nu}) \hat{x}_\theta(\Omega - \bar{\bar{\nu}}) | 0 \rangle d\nu \\
& + \Psi_m^2 \alpha^4 \int^\Omega \int^\Omega h(\nu - \Omega)^* h(\bar{\nu} - \Omega)^* \langle 0 | \hat{x}_\theta(\nu - \bar{\nu}) \hat{x}_\theta(\bar{\nu} - \bar{\bar{\nu}}) | 0 \rangle d\nu d\bar{\nu} \\
& + \Psi_m \alpha^2 \int^\Omega \int^\Omega h(\nu - \Omega)^* n_e(\bar{\nu})^* \langle 0 | \hat{x}_\theta(\nu - \bar{\nu}) \hat{x}_\theta(\bar{\nu} - \bar{\bar{\nu}}) | 0 \rangle d\nu d\bar{\nu} + \Psi_0 \Psi_m \alpha^2 \int^\Omega n_e(\nu)^* \langle 0 | \hat{x}_\theta(\nu - \bar{\nu}) \hat{x}_\theta(\Omega - \bar{\bar{\nu}}) | 0 \rangle d\nu d\bar{\nu} \\
& + \Psi_m \alpha^2 \int^\Omega \int^\Omega n_e(\nu)^* h(\bar{\nu} - \Omega)^* \langle 0 | \hat{x}_\theta(\nu - \bar{\nu}) \hat{x}_\theta(\bar{\nu} - \bar{\bar{\nu}}) | 0 \rangle d\nu d\bar{\nu} \\
& \left. + \int^\Omega \int^\Omega n_e(\nu)^* n_e(\bar{\nu})^* \langle 0 | \hat{x}_\theta(\nu - \bar{\nu}) \hat{x}_\theta(\bar{\nu} - \bar{\bar{\nu}}) | 0 \rangle d\nu d\bar{\nu} \right] d\bar{\nu} d\bar{\bar{\nu}} \right\rangle. \quad (31)
\end{aligned}$$

Using equation (20), this results in

$$\begin{aligned}
& \left\langle 2 \int \int \alpha(\bar{\nu}) \alpha(\bar{\bar{\nu}}) \int^\Omega \int^\Omega I(\nu)^* I(\bar{\nu})^* \hat{x}_\theta(\nu - \bar{\nu}) \hat{x}_\theta(\bar{\nu} - \bar{\bar{\nu}}) d\nu d\bar{\nu} d\bar{\bar{\nu}} \right\rangle \\
& = \frac{\Phi}{4} \Psi_0^2 \Psi_m^4 \alpha^6 + \frac{\Phi}{2} \Psi_0 \Psi_m^3 \alpha^4 \langle n_e(\Omega) \rangle + \frac{\Phi}{2} \Psi_m^3 \alpha^4 \int^0 \langle h(\nu) n_e(\Omega - \nu) \rangle d\nu + \frac{\Phi}{4} \Psi_m^2 \alpha^2 \int^\Omega \langle n_e(\nu) n_e(2\Omega - \nu) \rangle d\nu. \quad (32)
\end{aligned}$$

Similarly, we obtain

$$\begin{aligned} & \left\langle 2 \int \int \alpha(\bar{\nu})^* \alpha(\bar{\bar{\nu}})^* \int^\Omega \int^\Omega I(\nu) I(\bar{\nu}) \hat{x}_\theta(\nu - \bar{\nu})^\dagger \hat{x}_\theta(\bar{\nu} - \bar{\bar{\nu}})^\dagger d\nu d\bar{\nu} d\bar{\bar{\nu}} \right\rangle \\ &= \frac{\Phi}{4} \Psi_0^2 \Psi_m^4 \alpha^6 + \frac{\Phi}{2} \Psi_0 \Psi_m^3 \alpha^4 \langle n_e(\Omega)^* \rangle + \frac{\Phi}{2} \Psi_m^3 \alpha^4 \int^0 \langle h(\nu)^* n_e(\Omega - \nu)^* \rangle d\nu + \frac{\Phi}{4} \Psi_m^2 \alpha^2 \int^\Omega \langle n_e(\nu)^* n_e(2\Omega - \nu)^* \rangle d\nu. \quad (33) \end{aligned}$$

Using the same approach for term 5 of equation (28), we find

$$\begin{aligned} & \left\langle 4 \int \int \alpha(\bar{\nu}) \alpha(\bar{\bar{\nu}})^* \int^\Omega \int^\Omega I(\nu)^* I(\bar{\nu}) \hat{x}_\theta(\nu - \bar{\nu}) \hat{x}_\theta(\bar{\nu} - \bar{\bar{\nu}})^\dagger d\nu d\bar{\nu} d\bar{\bar{\nu}} \right\rangle \\ &= 2\Phi \Psi_0^4 \Psi_m^2 \alpha^6 + \Phi \Psi_0^2 \Psi_m^4 \alpha^6 + 2\Phi \Psi_0^2 \Psi_m^2 \alpha^6 \int \langle |h(\nu)|^2 \rangle d\nu + 4\Phi \Psi_0^2 \Psi_m^2 \alpha^6 \int^0 \langle |h(\bar{\nu})|^2 \rangle d\bar{\nu} \\ &+ 4\Phi \Psi_0^2 \Psi_m^2 \alpha^6 \int^0 \langle \Re[h(\bar{\nu})^2] \rangle d\bar{\nu} + 4\Phi \Psi_0 \Psi_m^2 \alpha^6 \int \int^\Omega \langle \Re[h(\bar{\nu} - \Omega) h(\bar{\bar{\nu}}) h(\Omega - \bar{\nu} - \bar{\bar{\nu}})^*] \rangle d\bar{\nu} d\bar{\bar{\nu}} \\ &+ 4\Phi \Psi_0^3 \Psi_m \alpha^4 \langle \Re[n_e(\Omega)] \rangle + 8\Phi \Psi_0^2 \Psi_m \alpha^4 \int^\Omega \langle \Re[n_e(\bar{\nu}) h(\bar{\nu} - \Omega)^*] \rangle d\bar{\nu} \\ &+ 4\Phi \Psi_0^2 \Psi_m \alpha^4 \int^\Omega \langle \Re[n_e(\bar{\nu}) h(\bar{\nu} - \Omega)] \rangle d\bar{\nu} + 2\Phi \Psi_0 \Psi_m^3 \alpha^4 \langle \Re[n_e(\Omega)] \rangle \\ &+ 4\Phi \Psi_0 \Psi_m \alpha^4 \int \int^\Omega \langle \Re[n_e(\bar{\nu}) h(\bar{\bar{\nu}}) h(\Omega - \bar{\nu} - \bar{\bar{\nu}})^*] \rangle d\bar{\nu} d\bar{\bar{\nu}} + 2\Phi \Psi_0^2 \Psi_m^2 \alpha^6 \int^0 \langle |h(\nu)|^2 \rangle d\nu \\ &+ 4\Phi \Psi_0 \Psi_m^2 \alpha^6 \int^\Omega \int^\Omega \langle \Re[h(\nu - \Omega)^* h(\bar{\nu} - \Omega) h(\bar{\nu} - \nu)^*] \rangle d\nu d\bar{\nu} + \Phi \Psi_m^4 \alpha^6 \int^0 \langle |h(\nu)|^2 \rangle d\nu \\ &+ 4\Phi \Psi_m^2 \alpha^6 \int \int \int^\Omega \int^\Omega \langle h(\nu - \Omega)^* h(\bar{\nu} - \Omega) h(\bar{\bar{\nu}})^* \hat{x}_\theta(\nu - \bar{\nu}) \hat{x}_\theta(\bar{\nu} - \bar{\bar{\nu}})^\dagger \rangle d\nu d\bar{\nu} d\bar{\bar{\nu}} \\ &+ 4\Phi \Psi_0 \Psi_m \alpha^4 \int^\Omega \int^\Omega \langle \Re[h(\nu - \Omega)^* n_e(\bar{\nu}) h(\bar{\nu} - \nu)^*] \rangle d\nu d\bar{\nu} \\ &+ 4\Phi \Psi_0 \Psi_m \alpha^4 \int^\Omega \int^\Omega \langle \Re[h(\nu - \Omega)^* n_e(\bar{\nu}) h(\nu - \bar{\nu})] \rangle d\nu d\bar{\nu} + 2\Phi \Psi_m^3 \alpha^4 \int^\Omega \langle \Re[h(\nu - \Omega)^* n_e(\nu)] \rangle d\nu \\ &+ 8\Phi \Psi_m \alpha^4 \int \int \int^\Omega \int^\Omega \langle \Re[h(\nu - \Omega)^* n_e(\bar{\nu}) h(\bar{\bar{\nu}})^*] \hat{x}_\theta(\nu - \bar{\nu}) \hat{x}_\theta(\bar{\nu} - \bar{\bar{\nu}})^\dagger \rangle d\nu d\bar{\nu} d\bar{\bar{\nu}} + 2\Phi \Psi_0^2 \alpha^2 \int^\Omega \langle |n_e(\nu)|^2 \rangle d\nu \\ &+ 4\Phi \Psi_0 \alpha^2 \int^\Omega \int^\Omega \langle \Re[n_e(\nu)^* n_e(\bar{\nu}) h(\bar{\nu} - \nu)^*] \rangle d\nu d\bar{\nu} + \Phi \Psi_m^2 \alpha^2 \int^\Omega \langle |n_e(\nu)|^2 \rangle d\nu \\ &+ 4\alpha^2 \int \int \int^\Omega \int^\Omega \langle n_e(\nu)^* n_e(\bar{\nu}) h(\bar{\bar{\nu}})^* \hat{x}_\theta(\nu - \bar{\nu}) \hat{x}_\theta(\bar{\nu} - \bar{\bar{\nu}})^\dagger \rangle d\nu d\bar{\nu} d\bar{\bar{\nu}}. \quad (34) \end{aligned}$$

For the calculation of term 6 of equation (27), we find

$$\begin{aligned} & \left\langle 2 \int \int \int^\Omega \int^\Omega |I(\nu)|^2 \hat{a}(\bar{\nu} - \bar{\bar{\nu}})^\dagger \hat{a}(-\bar{\bar{\nu}}) \hat{a}(-\bar{\bar{\nu}})^\dagger \hat{a}(\bar{\nu} - \bar{\bar{\nu}}) d\nu d\bar{\nu} d\bar{\bar{\nu}} \right\rangle \\ &= B\Lambda \left(\frac{\Phi^2}{4} + \frac{1}{4\Phi^2} - \frac{1}{2} \right) \int^\Omega \langle |I(\nu)|^2 \rangle d\nu \\ &= B\Lambda \left(\Psi_0^2 \Psi_m^2 \alpha^4 + 2\Psi_0 \Psi_m \alpha^2 \langle \Re[n_e(\Omega)] \rangle + \Psi_m^2 \alpha^4 \int^0 \langle |h(\nu)|^2 \rangle d\nu \right. \\ &\quad \left. + 2\Psi_m \alpha^2 \int^\Omega \langle \Re[h(\nu - \Omega)^* n_e(\nu)] \rangle d\nu + \int^\Omega \langle |n_e(\nu)|^2 \rangle d\nu \right) \left(\frac{\Phi^2}{4} + \frac{1}{4\Phi^2} - \frac{1}{2} \right). \quad (35) \end{aligned}$$

Similarly,

$$\begin{aligned}
& \left\langle \int \int \int \int^\Omega \int^\Omega I(\nu)^* I(\bar{\nu}) \hat{a}(-\bar{\nu})^\dagger \hat{a}(\nu - \bar{\nu}) \hat{a}(\bar{\nu} - \bar{\bar{\nu}})^\dagger \hat{a}(-\bar{\bar{\nu}}) d\nu d\bar{\nu} d\bar{\bar{\nu}} d\bar{\bar{\bar{\nu}}} \right\rangle \\
&= \left\langle \int \int \int \int^\Omega \int^\Omega I(\nu)^* I(\bar{\nu}) \hat{a}(\bar{\nu} - \bar{\bar{\nu}})^\dagger \hat{a}(-\bar{\bar{\nu}}) \hat{a}(-\bar{\nu})^\dagger \hat{a}(\nu - \bar{\nu}) d\nu d\bar{\nu} d\bar{\bar{\nu}} d\bar{\bar{\bar{\nu}}} \right\rangle \\
&= \Lambda \left(\Psi_0^2 \Psi_m^2 \alpha^4 + 2\Psi_0 \Psi_m \alpha^2 \langle \Re[n_e(\Omega)] \rangle + \Psi_m^2 \alpha^4 \int^0 \langle |h(\nu)|^2 \rangle d\nu \right. \\
&\quad \left. + 2\Psi_m \alpha^2 \int^\Omega \langle \Re[h(\nu - \Omega)^* n_e(\nu)] \rangle d\nu + \int^\Omega \langle |n_e(\nu)|^2 \rangle d\nu \right) \left(\frac{\Phi^2}{8} + \frac{1}{8\Phi^2} - \frac{1}{4} \right). \quad (36)
\end{aligned}$$

It is possible to combine terms 9-16 of equation (27) as follows:

$$\begin{aligned}
& 2 \int \int \int \int^\Omega \int^\Omega \left[\langle I(\nu)^* \alpha(\bar{\nu}) \alpha(\bar{\bar{\nu}})^* \hat{x}_\theta(\nu - \bar{\nu}) \hat{x}_\theta(\bar{\nu} - \bar{\bar{\nu}})^\dagger \hat{a}(-\bar{\bar{\nu}})^\dagger \hat{a}(\bar{\nu} - \bar{\bar{\bar{\nu}}}) \rangle \right. \\
&+ \langle I(\nu)^* \alpha(\bar{\nu}) \alpha(\bar{\bar{\nu}})^* \hat{x}_\theta(\bar{\nu} - \bar{\bar{\bar{\nu}}})^\dagger \hat{a}(-\bar{\bar{\bar{\nu}}})^\dagger \hat{a}(\bar{\nu} - \bar{\bar{\bar{\nu}}}) \hat{x}_\theta(\nu - \bar{\nu}) \rangle + \langle I(\nu)^* \alpha(\bar{\nu})^* \alpha(\bar{\bar{\nu}}) \hat{a}(-\bar{\bar{\nu}})^\dagger \hat{a}(\nu - \bar{\bar{\nu}}) \hat{x}_\theta(\bar{\nu} - \bar{\bar{\nu}})^\dagger \hat{x}_\theta(\bar{\nu} - \bar{\bar{\bar{\nu}}}) \rangle \\
&+ \langle I(\nu)^* \alpha(\bar{\nu})^* \alpha(\bar{\bar{\nu}}) \hat{x}_\theta(\bar{\nu} - \bar{\bar{\nu}})^\dagger \hat{x}_\theta(\bar{\nu} - \bar{\bar{\bar{\nu}}}) \hat{a}(-\bar{\bar{\nu}})^\dagger \hat{a}(\nu - \bar{\bar{\nu}}) \rangle + \langle I(\nu) \alpha(\bar{\nu})^* \alpha(\bar{\bar{\nu}}) \hat{x}_\theta(\nu - \bar{\nu})^\dagger \hat{a}(\bar{\nu} - \bar{\bar{\nu}})^\dagger \hat{a}(-\bar{\bar{\bar{\nu}}}) \hat{x}_\theta(\bar{\nu} - \bar{\bar{\bar{\nu}}}) \rangle \\
&+ \langle I(\nu) \alpha(\bar{\nu})^* \alpha(\bar{\bar{\nu}}) \hat{a}(\bar{\nu} - \bar{\bar{\bar{\nu}}})^\dagger \hat{a}(-\bar{\bar{\bar{\nu}}}) \hat{x}_\theta(\bar{\nu} - \bar{\bar{\bar{\nu}}}) \hat{x}_\theta(\nu - \bar{\nu})^\dagger \rangle + \langle I(\nu) \alpha(\bar{\nu})^* \alpha(\bar{\bar{\nu}}) \hat{x}_\theta(\bar{\nu} - \bar{\bar{\nu}})^\dagger \hat{x}_\theta(\bar{\nu} - \bar{\bar{\bar{\nu}}}) \hat{a}(\nu - \bar{\bar{\nu}})^\dagger \hat{a}(-\bar{\bar{\bar{\nu}}}) \rangle \\
&\quad \left. + \langle I(\nu) \alpha(\bar{\nu})^* \alpha(\bar{\bar{\nu}}) \hat{a}(\nu - \bar{\bar{\bar{\nu}}})^\dagger \hat{a}(-\bar{\bar{\bar{\nu}}}) \hat{x}_\theta(\bar{\nu} - \bar{\bar{\bar{\nu}}})^\dagger \hat{x}_\theta(\bar{\nu} - \bar{\bar{\bar{\nu}}}) \rangle \right] d\nu d\bar{\nu} d\bar{\bar{\nu}} d\bar{\bar{\bar{\nu}}} \\
&= (4\Phi^2 - 2) \int \int \int^\Omega \int^\Omega \langle \Re[I(\nu)] \alpha(\bar{\nu}) \alpha(\bar{\bar{\nu}} - \nu)^* \rangle d\nu d\bar{\nu} d\bar{\bar{\nu}} \\
&= (4\Phi^2 - 2) \left[\Psi_0^2 \Psi_m^2 \alpha^4 B + \Psi_m^2 \alpha^4 B \int^0 \langle \Re[h(\nu)]^2 \rangle d\nu \right. \\
&\quad \left. + \Psi_0 \Psi_m \alpha^2 B \langle \Re[n_e(\Omega)] \rangle + \Psi_m \alpha^2 B \int^\Omega \langle \Re[n_e(\nu)] \Re[h(\nu - \Omega)] \rangle d\nu \right] \quad (37)
\end{aligned}$$

Similarly, we find that terms 17-20 of equation (27) simplify as

$$\begin{aligned}
& 2 \int \int \int \int^\Omega \int^\Omega \left[\langle I(\nu)^* \alpha(\bar{\nu}) \alpha(\bar{\bar{\nu}}) \hat{x}_\theta(\nu - \bar{\nu}) \hat{a}(\bar{\nu} - \bar{\bar{\bar{\nu}}})^\dagger \hat{a}(-\bar{\bar{\bar{\nu}}}) \hat{x}_\theta(\bar{\nu} - \bar{\bar{\bar{\nu}}}) \rangle \right. \\
&+ \langle I(\nu)^* \alpha(\bar{\nu}) \alpha(\bar{\bar{\nu}}) \hat{a}(\bar{\nu} - \bar{\bar{\bar{\nu}}})^\dagger \hat{a}(-\bar{\bar{\bar{\nu}}}) \hat{x}_\theta(\bar{\nu} - \bar{\bar{\bar{\nu}}}) \hat{x}_\theta(\nu - \bar{\nu}) \rangle \\
&+ \langle I(\nu) \alpha(\bar{\nu})^* \alpha(\bar{\bar{\nu}})^* \hat{x}_\theta(\nu - \bar{\nu})^\dagger \hat{x}_\theta(\bar{\nu} - \bar{\bar{\nu}})^\dagger \hat{a}(-\bar{\bar{\nu}})^\dagger \hat{a}(\bar{\nu} - \bar{\bar{\bar{\nu}}}) \hat{x}_\theta(\bar{\nu} - \bar{\bar{\bar{\nu}}}) \rangle \\
&\quad \left. + \langle I(\nu) \alpha(\bar{\nu})^* \alpha(\bar{\bar{\nu}})^* \hat{x}_\theta(\bar{\nu} - \bar{\bar{\bar{\nu}}})^\dagger \hat{a}(-\bar{\bar{\bar{\nu}}})^\dagger \hat{x}_\theta(\bar{\nu} - \bar{\bar{\bar{\nu}}}) \hat{x}_\theta(\nu - \bar{\nu})^\dagger \right] d\nu d\bar{\nu} d\bar{\bar{\nu}} d\bar{\bar{\bar{\nu}}} \\
&= 2\Phi^2 \int \int \int^\Omega \int^\Omega \langle \Re[I(\nu) \alpha(\bar{\nu})^* \alpha(\nu - \bar{\bar{\nu}})^*] \rangle d\nu d\bar{\nu} d\bar{\bar{\nu}} \\
&= 2\Phi^2 \Psi_0^2 \Psi_m^2 \alpha^4 B + 2\Phi^2 \Psi_m^2 \alpha^4 B \int^0 \langle |h(\nu)|^2 \rangle d\nu \\
&\quad + 2\Phi^2 \Psi_0 \Psi_m \alpha^2 B \langle \Re[n_e(\Omega)] \rangle + 2\Phi^2 \Psi_m \alpha^2 B \int^\Omega \langle \Re[n_e(\nu) h(\nu - \Omega)^*] \rangle d\nu. \quad (38)
\end{aligned}$$

We can write term 21 of equation (27) as

$$\begin{aligned}
& 4 \int \int \int \int \int^\Omega \int^\Omega \langle \alpha(\bar{\nu})^* \alpha(\bar{\bar{\nu}}) \alpha(\bar{\bar{\bar{\nu}}})^* \alpha(\bar{\bar{\bar{\bar{\nu}}}}) \hat{x}_\theta(\nu - \bar{\nu})^\dagger \hat{x}_\theta(\nu - \bar{\bar{\nu}}) \hat{x}_\theta(\bar{\nu} - \bar{\bar{\bar{\nu}}})^\dagger \hat{x}_\theta(\bar{\nu} - \bar{\bar{\bar{\bar{\nu}}}}) \rangle d\nu d\bar{\nu} d\bar{\bar{\nu}} d\bar{\bar{\bar{\nu}}} d\bar{\bar{\bar{\bar{\nu}}}} \\
&= 4 \int^\Omega \int^\Omega \left| \int \alpha(\bar{\nu}) \hat{x}_\theta(\nu - \bar{\bar{\nu}}) d\bar{\nu} \right|^2 \left| \int \alpha(\bar{\bar{\nu}}) \hat{x}_\theta(\bar{\nu} - \bar{\bar{\bar{\nu}}}) d\bar{\bar{\nu}} \right|^2 d\nu d\bar{\nu}
\end{aligned}$$

$$= 4 \int^{\Omega} \int^{\Omega} \left| \Psi_0 \alpha \hat{x}_{\theta}(\nu) + \frac{\Psi_m \alpha}{2} [\hat{x}_{\theta}(\nu - \Omega) + \hat{x}_{\theta}(\nu + \Omega)] + \alpha \int h(\bar{\nu}) \hat{x}_{\theta}(\nu - \bar{\nu}) d\bar{\nu} \right|^2 \\ \left| \Psi_0 \alpha \hat{x}_{\theta}(\bar{\nu}) + \frac{\Psi_m \alpha}{2} [\hat{x}_{\theta}(\bar{\nu} - \Omega) + \hat{x}_{\theta}(\bar{\nu} + \Omega)] + \alpha \int h(\bar{\bar{\nu}}) \hat{x}_{\theta}(\bar{\nu} - \bar{\bar{\nu}}) d\bar{\bar{\nu}} \right|^2 d\nu d\bar{\nu}. \quad (39)$$

In the expansion of equation (39), many terms vanish due to both the restricted domain of $h(\nu)$ and the action of creation and annihilation operators on the vacuum. This allows equation (39) to be significantly simplified, leading to the result:

$$4 \int \int \int \int \int^{\Omega} \int^{\Omega} \langle \alpha(\bar{\nu})^* \alpha(\bar{\bar{\nu}}) \alpha(\bar{\bar{\bar{\nu}}})^* \alpha(\bar{\bar{\bar{\bar{\nu}}}}) \hat{x}_{\theta}(\nu - \bar{\nu})^{\dagger} \hat{x}_{\theta}(\nu - \bar{\bar{\nu}}) \hat{x}_{\theta}(\bar{\nu} - \bar{\bar{\nu}})^{\dagger} \hat{x}_{\theta}(\bar{\nu} - \bar{\bar{\bar{\nu}}}) \rangle d\nu d\bar{\nu} d\bar{\bar{\nu}} d\bar{\bar{\bar{\nu}}} d\bar{\bar{\bar{\bar{\nu}}}} \\ = \Phi^2 \Psi_0^4 \alpha^4 B^2 + \Phi^2 \Psi_0^4 \alpha^4 B + \Phi^2 \Psi_0^2 \alpha^4 B \int \langle |h(\bar{\nu})|^2 \rangle d\bar{\nu} + \Phi^2 \Psi_0^2 \alpha^4 B \int \langle \Re[h(\bar{\nu})^2] \rangle d\bar{\nu} \\ + 3\Phi^2 \Psi_0^2 \alpha^4 \int^{\Omega} \int^{\Omega} \langle |h(\nu - \bar{\nu})|^2 \rangle d\nu d\bar{\nu} + \Phi^2 \Psi_0^2 \alpha^4 \int^{\Omega} \int^{\Omega} \langle \Re[h(\nu - \bar{\nu})^2] \rangle d\nu d\bar{\nu} + \Phi^2 \Psi_0^2 \Psi_m^2 \alpha^4 B^2 \\ + 2\Phi^2 \Psi_0^2 \alpha^4 B^2 \int \langle |h(\bar{\nu})|^2 \rangle d\bar{\nu} + \frac{\Psi_m^4 \alpha^4 \Phi^2 B^2}{4} + \frac{\Psi_m^4 \alpha^4 \Phi^2 B}{2} + \Psi_m^2 \alpha^4 \Phi^2 B^2 \int \langle |h(\bar{\nu})|^2 \rangle d\bar{\nu} \\ + \Phi^2 \alpha^4 B^2 \int \int \langle |h(\bar{\nu})|^2 |h(\bar{\bar{\nu}})|^2 \rangle d\bar{\nu} d\bar{\bar{\nu}} + \Phi^2 \alpha^4 \int \int \int^{\Omega} \int^{\Omega} \langle h(\bar{\nu}) h(\bar{\bar{\nu}})^* h(\bar{\nu} + \bar{\bar{\nu}} - \nu) h(\bar{\nu} + \bar{\bar{\nu}} - \nu)^* \rangle d\nu d\bar{\nu} d\bar{\bar{\nu}} d\bar{\bar{\bar{\nu}}}. \quad (40)$$

The summation of terms 22-27 of equation (27) can be written as

$$2 \int \int \int \int \int^{\Omega} \int^{\Omega} \left[\langle \alpha(\bar{\nu})^* \alpha(\bar{\bar{\nu}}) \hat{x}_{\theta}(\nu - \bar{\nu})^{\dagger} \hat{x}_{\theta}(\nu - \bar{\bar{\nu}}) \hat{a}(\bar{\nu} - \bar{\bar{\nu}})^{\dagger} \hat{a}(-\bar{\bar{\nu}}) \hat{a}(-\bar{\bar{\bar{\nu}}})^{\dagger} \hat{a}(\bar{\nu} - \bar{\bar{\bar{\nu}}}) \rangle \right. \\ + \langle \alpha(\bar{\nu})^* \alpha(\bar{\bar{\nu}}) \hat{a}(\bar{\nu} - \bar{\bar{\nu}})^{\dagger} \hat{a}(-\bar{\bar{\nu}}) \hat{a}(-\bar{\bar{\bar{\nu}}})^{\dagger} \hat{a}(\bar{\nu} - \bar{\bar{\bar{\nu}}}) \hat{x}_{\theta}(\nu - \bar{\nu})^{\dagger} \hat{x}_{\theta}(\nu - \bar{\bar{\nu}}) \rangle \\ + \langle \alpha(\bar{\nu})^* \alpha(\bar{\bar{\nu}}) \hat{x}_{\theta}(\nu - \bar{\nu})^{\dagger} \hat{a}(-\bar{\bar{\nu}})^{\dagger} \hat{a}(\nu - \bar{\bar{\nu}}) \hat{a}(\bar{\nu} - \bar{\bar{\bar{\nu}}})^{\dagger} \hat{a}(-\bar{\bar{\bar{\nu}}}) \hat{x}_{\theta}(\bar{\nu} - \bar{\bar{\nu}}) \rangle \\ \left. + \langle \alpha(\bar{\nu})^* \alpha(\bar{\bar{\nu}}) \hat{a}(\bar{\nu} - \bar{\bar{\bar{\nu}}})^{\dagger} \hat{a}(-\bar{\bar{\bar{\nu}}}) \hat{x}_{\theta}(\bar{\nu} - \bar{\bar{\bar{\nu}}}) \hat{x}_{\theta}(\nu - \bar{\bar{\nu}})^{\dagger} \hat{a}(-\bar{\bar{\bar{\nu}}})^{\dagger} \hat{a}(\nu - \bar{\bar{\bar{\nu}}}) \rangle \right] d\nu d\bar{\nu} d\bar{\bar{\nu}} d\bar{\bar{\bar{\nu}}} d\bar{\bar{\bar{\bar{\nu}}}} \\ = B^2 \left[\frac{5\Phi^3}{2} - 2\Phi + \frac{1}{2\Phi} \right] \int \langle |\alpha(\bar{\nu})|^2 \rangle d\bar{\nu} \\ = B^2 \left[\frac{5\Phi^3}{2} - 2\Phi + \frac{1}{2\Phi} \right] \left(\Psi_0^2 \alpha^2 + \frac{\Psi_m^2 \alpha^2}{2} + \alpha^2 \int \langle |h(\bar{\nu})|^2 \rangle d\bar{\nu} \right). \quad (41)$$

Similarly, we can combine terms 26 and 27 of equation (27) to give

$$2 \int \int \int \int \int^{\Omega} \int^{\Omega} \left[\langle \alpha(\bar{\nu})^* \alpha(\bar{\bar{\nu}})^* \hat{x}_{\theta}(\nu - \bar{\nu})^{\dagger} \hat{a}(-\bar{\bar{\nu}}) \hat{a}(\nu - \bar{\bar{\nu}}) \hat{x}_{\theta}(\bar{\nu} - \bar{\bar{\nu}})^{\dagger} \hat{a}(-\bar{\bar{\bar{\nu}}})^{\dagger} \hat{a}(\bar{\nu} - \bar{\bar{\bar{\nu}}}) \rangle \right. \\ + \langle \alpha(\bar{\nu}) \alpha(\bar{\bar{\nu}}) \hat{a}(\nu - \bar{\bar{\bar{\nu}}})^{\dagger} \hat{a}(-\bar{\bar{\bar{\nu}}}) \hat{x}_{\theta}(\nu - \bar{\bar{\nu}}) \hat{a}(\bar{\nu} - \bar{\bar{\bar{\nu}}})^{\dagger} \hat{a}(-\bar{\bar{\bar{\nu}}}) \hat{x}_{\theta}(\bar{\nu} - \bar{\bar{\nu}}) \rangle \left. \right] d\nu d\bar{\nu} d\bar{\bar{\nu}} d\bar{\bar{\bar{\nu}}} d\bar{\bar{\bar{\bar{\nu}}}} \\ = B^2 [\Phi^3 - \Phi] \left(\Psi_0^2 \alpha^2 + \frac{\Psi_m^2 \alpha^2}{2} + \alpha^2 \int \langle \Re[h(\bar{\nu})^2] \rangle d\bar{\nu} \right). \quad (42)$$

The final term of equation (27) gives the result

$$\int \int \int \int \int^{\Omega} \int^{\Omega} \langle \hat{a}(\nu - \bar{\nu})^{\dagger} \hat{a}(-\bar{\nu}) \hat{a}(-\bar{\bar{\nu}})^{\dagger} \hat{a}(\nu - \bar{\bar{\nu}}) \hat{a}(\bar{\nu} - \bar{\bar{\bar{\nu}}})^{\dagger} \hat{a}(-\bar{\bar{\bar{\nu}}}) \hat{a}(-\bar{\bar{\bar{\bar{\nu}}}})^{\dagger} \hat{a}(\bar{\nu} - \bar{\bar{\bar{\bar{\nu}}}}) \rangle d\nu d\bar{\nu} d\bar{\bar{\nu}} d\bar{\bar{\bar{\nu}}} d\bar{\bar{\bar{\bar{\nu}}}} \\ = B^2 \Lambda \left(\frac{7\Phi^4}{32} - \frac{3\Phi^2}{8} + \frac{7}{32\Phi^4} - \frac{3}{8\Phi^2} + \frac{5}{16} \right). \quad (43)$$

By combining all the terms calculated for equation (27), we obtain the result for $\langle p_\Omega^2 \rangle$:

$$\begin{aligned}
\langle p_\Omega^2 \rangle = & 4q^4 R^2 \left[\alpha^8 \left[\Psi_0^4 \Psi_m^4 + 2\Psi_0^2 \Psi_m^4 \int^0 \langle |h(\nu)|^2 \rangle d\nu + \Psi_m^4 \int^0 \int^0 \langle |h(\nu)|^2 |h(\bar{\nu})|^2 \rangle d\nu d\bar{\nu} \right] \right. \\
& + \alpha^6 \left[4\Psi_0^3 \Psi_m^3 \langle \Re[n_e(\Omega)] \rangle + 4\Psi_0^2 \Psi_m^3 \int^\Omega \langle \Re[h(\nu - \Omega)^* n_e(\nu)] \rangle d\nu + 4\Psi_0 \Psi_m^3 \int^0 \langle \Re[n_e(\Omega)] |h(\nu)|^2 \rangle d\nu \right. \\
& + 4\Psi_m^3 \int^\Omega \int^0 \langle |h(\nu)|^2 \Re[h(\bar{\nu} - \Omega)^* n_e(\bar{\nu})] \rangle d\nu d\bar{\nu} + 2\Phi B \Psi_0^4 \Psi_m^2 + \Phi B \Psi_0^2 \Psi_m^4 + 2\Phi B \Psi_0^2 \Psi_m^2 \int \langle |h(\bar{\nu})|^2 \rangle d\bar{\nu} \\
& + 2\Phi B \Psi_0^2 \Psi_m^2 \int^0 \langle |h(\nu)|^2 \rangle d\nu + \Phi B \Psi_m^4 \int^0 \langle |h(\nu)|^2 \rangle d\nu + 2\Phi B \Psi_m^2 \int \int^0 \langle |h(\nu)|^2 |h(\bar{\nu})|^2 \rangle d\nu d\bar{\nu} \\
& + 2\Phi \Psi_0^4 \Psi_m^2 + \frac{3}{2} \Phi \Psi_0^2 \Psi_m^4 + 2\Phi \Psi_0^2 \Psi_m^2 \int \langle |h(\nu)|^2 \rangle d\nu + 4\Phi \Psi_0^2 \Psi_m^2 \int^0 \langle |h(\bar{\nu})|^2 \rangle d\bar{\nu} \\
& + 4\Phi \Psi_0^2 \Psi_m^2 \int^0 \langle \Re[h(\bar{\nu})^2] \rangle d\bar{\nu} + 4\Phi \Psi_0 \Psi_m^2 \int \int^\Omega \langle \Re[h(\bar{\nu} - \Omega) h(\bar{\nu}) h(\Omega - \bar{\nu} - \bar{\nu})^*] \rangle d\bar{\nu} d\bar{\nu} \\
& + 2\Phi \Psi_0^2 \Psi_m^2 \int^0 \langle |h(\nu)|^2 \rangle d\nu + 4\Phi \Psi_0 \Psi_m^2 \int^\Omega \int^\Omega \langle \Re[h(\nu - \Omega)^* h(\bar{\nu} - \Omega) h(\bar{\nu} - \nu)^*] \rangle d\nu d\bar{\nu} \\
& + \Phi \Psi_m^4 \int^0 \langle |h(\nu)|^2 \rangle d\nu + 4\Psi_m^2 \int \int \int^\Omega \int^\Omega \langle h(\nu - \Omega)^* h(\bar{\nu} - \Omega) h(\bar{\nu}) h(\bar{\bar{\nu}})^* \hat{x}_\theta(\nu - \bar{\nu}) \hat{x}_\theta(\bar{\nu} - \bar{\bar{\nu}})^\dagger \rangle d\nu d\bar{\nu} d\bar{\bar{\nu}} d\bar{\bar{\bar{\nu}}} \left. \right] \\
& + \alpha^4 \left[2\Psi_0^2 \Psi_m^2 \int^\Omega \langle |n_e(\nu)|^2 \rangle d\nu + 4\Psi_0^2 \Psi_m^2 \langle \Re[n_e(\Omega)]^2 \rangle + 8\Psi_0 \Psi_m^2 \int^\Omega \langle \Re[h(\nu - \Omega)^* n_e(\nu)] \Re[n_e(\Omega)] \rangle d\nu \right. \\
& + 2\Psi_m^2 \int^\Omega \int^0 \langle |h(\nu)|^2 |n_e(\bar{\nu})|^2 \rangle d\nu d\bar{\nu} + 4\Psi_m^2 \int^\Omega \int^\Omega \langle \Re[h(\nu - \Omega)^* n_e(\nu)] \Re[h(\bar{\nu} - \Omega)^* n_e(\bar{\nu})] \rangle d\nu d\bar{\nu} \\
& + 4\Phi B \Psi_0^3 \Psi_m \langle \Re[n_e(\Omega)] \rangle + 2\Phi B \Psi_0 \Psi_m^3 \langle \Re[n_e(\Omega)] \rangle + 4\Phi B \Psi_0 \Psi_m \int \langle \Re[n_e(\Omega)] |h(\bar{\nu})|^2 \rangle d\bar{\nu} \\
& + 4\Phi B \Psi_0^2 \Psi_m \int^\Omega \langle \Re[h(\nu - \Omega)^* n_e(\nu)] \rangle d\nu + 2\Phi B \Psi_m^3 \int^\Omega \langle \Re[h(\nu - \Omega)^* n_e(\nu)] \rangle d\nu \\
& + 4\Phi B \Psi_m \int \int^\Omega \langle \Re[h(\nu - \Omega)^* n_e(\nu)] |h(\bar{\nu})|^2 \rangle d\nu d\bar{\nu} + \Phi \Psi_m^3 \int^0 \langle \Re[h(\nu) n_e(\Omega - \nu)] \rangle d\nu \\
& + 4\Phi \Psi_0^3 \Psi_m \langle \Re[n_e(\Omega)] \rangle + 8\Phi \Psi_0^2 \Psi_m \int^\Omega \langle \Re[n_e(\bar{\nu}) h(\bar{\nu} - \Omega)^*] \rangle d\bar{\nu} + 4\Phi \Psi_0^2 \Psi_m \int^\Omega \langle \Re[n_e(\bar{\nu}) h(\bar{\nu} - \Omega)] \rangle d\bar{\nu} \\
& + 3\Phi \Psi_0 \Psi_m^3 \langle \Re[n_e(\Omega)] \rangle + 4\Phi \Psi_0 \Psi_m \int \int^\Omega \langle \Re[n_e(\bar{\nu}) h(\bar{\nu}) h(\Omega - \bar{\nu} - \bar{\nu})^*] \rangle d\bar{\nu} d\bar{\bar{\nu}} \\
& + 4\Phi \Psi_0 \Psi_m \int^\Omega \int^\Omega \langle \Re[h(\nu - \Omega)^* n_e(\bar{\nu}) h(\bar{\nu} - \nu)^*] \rangle d\nu d\bar{\nu} \\
& + 4\Phi \Psi_0 \Psi_m \int^\Omega \int^\Omega \langle \Re[h(\nu - \Omega)^* n_e(\bar{\nu}) h(\nu - \bar{\nu})] \rangle d\nu d\bar{\nu} + 2\Phi \Psi_m^3 \int^\Omega \langle \Re[h(\nu - \Omega)^* n_e(\nu)] \rangle d\nu \\
& + 8\Psi_m \int \int \int^\Omega \int^\Omega \langle \Re[h(\nu - \Omega)^* n_e(\bar{\nu}) h(\bar{\nu}) h(\bar{\bar{\nu}})^*] \hat{x}_\theta(\nu - \bar{\nu}) \hat{x}_\theta(\bar{\nu} - \bar{\bar{\nu}})^\dagger \rangle d\nu d\bar{\nu} d\bar{\bar{\nu}} d\bar{\bar{\bar{\nu}}} \\
& + (B + 1) \Psi_m^2 \Lambda \left(\frac{\Phi^2}{4} + \frac{1}{4\Phi^2} - \frac{1}{2} \right) \int^0 \langle |h(\nu)|^2 \rangle d\nu + (B + 1) \Psi_0^2 \Psi_m^2 \Lambda \left(\frac{\Phi^2}{4} + \frac{1}{4\Phi^2} - \frac{1}{2} \right) \\
& + (6\Phi^2 - 2) \Psi_0^2 \Psi_m^2 B + (4\Phi^2 - 2) \Psi_m^2 B \int^0 \langle \Re[h(\nu)]^2 \rangle d\nu + 2\Phi^2 \Psi_m^2 B \int^0 \langle |h(\nu)|^2 \rangle d\nu + \Phi^2 \Psi_0^4 B^2 + \Phi^2 \Psi_0^4 B \\
& + \Phi^2 \Psi_0^2 B \int \langle |h(\bar{\nu})|^2 \rangle d\bar{\nu} + \Phi^2 \Psi_0^2 B \int \langle \Re[h(\bar{\nu})^2] \rangle d\bar{\nu} + 3\Phi^2 \Psi_0^2 \int^\Omega \int^\Omega \langle |h(\nu - \bar{\nu})|^2 \rangle d\nu d\bar{\nu} \\
& + \Phi^2 \Psi_0^2 \int^\Omega \int^\Omega \langle \Re[h(\nu - \bar{\nu})^2] \rangle d\nu d\bar{\nu} + \Phi^2 \Psi_0^2 \Psi_m^2 B^2 + 2\Phi^2 \Psi_0^2 B^2 \int \langle |h(\bar{\nu})|^2 \rangle d\bar{\nu} + \frac{\Psi_m^4 \Phi^2 B^2}{4}
\end{aligned}$$

$$\begin{aligned}
& + \frac{\Psi_m^4 \Phi^2 B}{2} + \Psi_m^2 \Phi^2 B^2 \int \langle |h(\bar{\nu})|^2 \rangle d\bar{\nu} + \Phi^2 B^2 \int \int \langle |h(\bar{\nu})|^2 |h(\bar{\bar{\nu}})|^2 \rangle d\bar{\nu} d\bar{\bar{\nu}} \\
& + \Phi^2 \int \int \int \int \langle h(\bar{\nu}) h(\bar{\bar{\nu}})^* h(\bar{\nu} + \bar{\bar{\nu}} - \nu) h(\bar{\nu} + \bar{\bar{\nu}} - \nu)^* \rangle d\nu d\bar{\nu} d\bar{\bar{\nu}} d\bar{\bar{\bar{\nu}}} \Big] \\
& + \alpha^2 \left[4\Psi_0 \Psi_m \int^\Omega \langle |n_e(\nu)|^2 \Re[n_e(\Omega)] \rangle d\nu + 4\Psi_m \int^\Omega \int^\Omega \langle \Re[h(\nu - \Omega)^* n_e(\nu)] |n_e(\bar{\nu})|^2 \rangle d\nu d\bar{\nu} \right. \\
& + 2\Phi B \Psi_0^2 \int^\Omega \langle |n_e(\nu)|^2 \rangle d\nu + \Phi B \Psi_m^2 \int^\Omega \langle |n_e(\nu)|^2 \rangle d\nu + 2\Phi B \int^\Omega \int^\Omega \langle |n_e(\nu)|^2 |h(\bar{\nu})|^2 \rangle d\nu d\bar{\nu} \\
& + \frac{\Phi}{2} \Psi_m^2 \int^\Omega \langle \Re[n_e(\nu) n_e(2\Omega - \nu)] \rangle d\nu + 2\Phi \Psi_0^2 \int^\Omega \langle |n_e(\nu)|^2 \rangle d\nu \\
& + 4\Phi \Psi_0 \int^\Omega \int^\Omega \langle \Re[n_e(\nu)^* n_e(\bar{\nu}) h(\bar{\nu} - \nu)^*] \rangle d\nu d\bar{\nu} + \Phi \Psi_m^2 \int^\Omega \langle |n_e(\nu)|^2 \rangle d\nu \\
& + 4 \int \int \int \int \langle n_e(\nu)^* n_e(\bar{\nu}) h(\bar{\bar{\nu}}) h(\bar{\bar{\bar{\nu}}})^* \hat{x}_\theta(\nu - \bar{\nu}) \hat{x}_\theta(\bar{\nu} - \bar{\bar{\nu}})^\dagger \rangle d\nu d\bar{\nu} d\bar{\bar{\nu}} d\bar{\bar{\bar{\nu}}} \\
& + (B+1)\Psi_0 \Psi_m \langle \Re[n_e(\Omega)] \rangle \Lambda \left(\frac{\Phi^2}{2} + \frac{1}{2\Phi^2} - 1 \right) + (B+1)\Psi_m \Lambda \left(\frac{\Phi^2}{2} + \frac{1}{2\Phi^2} - 1 \right) \int^\Omega \langle \Re[h(\nu - \Omega)^* n_e(\nu)] \rangle d\nu \\
& + (6\Phi^2 - 2)\Psi_0 \Psi_m B \langle \Re[n_e(\Omega)] \rangle + (4\Phi^2 - 2)\Psi_m B \int^\Omega \langle \Re[n_e(\nu)] \Re[h(\nu - \Omega)] \rangle d\nu \\
& + 2\Phi^2 \Psi_m B \int^\Omega \langle \Re[n_e(\nu) h(\nu - \Omega)^*] \rangle d\nu + B^2 \Psi_0^2 \left[\frac{7\Phi^3}{2} - 3\Phi + \frac{1}{2\Phi} \right] + B^2 \Psi_m^2 \left[\frac{7\Phi^3}{4} - \frac{3}{2}\Phi + \frac{1}{4\Phi} \right] \\
& + B^2 \left[\frac{5\Phi^3}{2} - 2\Phi + \frac{1}{2\Phi} \right] \int \langle |h(\bar{\nu})|^2 \rangle d\bar{\nu} + B^2 [\Phi^3 - \Phi] \int \langle \Re[h(\bar{\nu})^2] \rangle d\bar{\nu} \Big] + \int^\Omega \int^\Omega \langle |n_e(\nu)|^2 |n_e(\bar{\nu})|^2 \rangle d\nu d\bar{\nu} \\
& + (B+1)\Lambda \left(\frac{\Phi^2}{4} + \frac{1}{4\Phi^2} - \frac{1}{2} \right) \int^\Omega \langle |n_e(\nu)|^2 \rangle d\nu \\
& + B^2 \Lambda \left(\frac{7\Phi^4}{32} - \frac{3\Phi^2}{8} + \frac{7}{32\Phi^4} - \frac{3}{8\Phi^2} + \frac{5}{16} \right) \Big]. \quad (44)
\end{aligned}$$

Due to the cancellation of terms in the expression for $\text{Var}(p_\Omega) = \langle p_\Omega^2 \rangle - \langle p_\Omega \rangle^2$, and by taking the leading terms we find that

$$\begin{aligned}
\text{Var}(p_\Omega) = \langle p_\Omega^2 \rangle - \langle p_\Omega \rangle^2 & \approx \Psi_m^4 \alpha^8 \left[\int^0 \int^0 \langle |h(\nu)|^2 |h(\bar{\nu})|^2 \rangle d\nu d\bar{\nu} - \int^0 \int^0 \langle |h(\nu)|^2 \rangle \langle |h(\bar{\nu})|^2 \rangle d\nu d\bar{\nu} \right] \\
& + 2\Phi B \Psi_m^2 \alpha^6 \left[\int \int \langle |h(\nu)|^2 |h(\bar{\nu})|^2 \rangle d\nu d\bar{\nu} - \int \int \langle |h(\nu)|^2 \rangle \langle |h(\bar{\nu})|^2 \rangle d\nu d\bar{\nu} \right] \\
& + 2\Phi \Psi_0^4 \Psi_m^2 \alpha^6 + \int^\Omega \int^\Omega \langle |n_e(\nu)|^2 |n_e(\bar{\nu})|^2 \rangle d\nu d\bar{\nu} - \int^\Omega \int^\Omega \langle |n_e(\nu)|^2 \rangle \langle |n_e(\bar{\nu})|^2 \rangle d\nu d\bar{\nu}. \quad (45)
\end{aligned}$$

By associating $\mathcal{H}_0 = \int^0 |h(\nu)|^2 d\nu$ as the classical optical noise in the DC component, $\mathcal{H} = \int |h(\nu)|^2 d\nu$ as the total classical optical noise, $\mathcal{N} = \int^\Omega |n_e(\nu)|^2 d\nu$ as the electronic noise in the $\pm B$ frequency interval around Ω , and substituting $\Psi_0 \approx 1$, $\Psi_m = \delta_m/2$ and $i_0 = q\eta\alpha_0^2$, we find that

$$\text{Var}(p_\Omega) \approx R^2 \left[2\Phi q \delta_m^2 i_0^3 [\text{Cov}(\mathcal{H}_0, \mathcal{H}) B + 1] + \frac{\delta_m^4 i_0^4}{4} \text{Var}(\mathcal{H}_0) + 4q^4 \text{Var}(\mathcal{N}) \right], \quad (46)$$

where

$$\text{Cov}(\mathcal{H}_0, \mathcal{H}) = \langle \mathcal{H}_0 \mathcal{H} \rangle - \langle \mathcal{H}_0 \rangle \langle \mathcal{H} \rangle \quad (47)$$

is to the covariance between \mathcal{H}_0 and \mathcal{H} . The condition $\text{Cov}(\mathcal{H}_0, \mathcal{H}) > \text{Var}(\mathcal{H}_0)$ is satisfied when there are significant spectral correlations in the classical noise. From [34], we expect this to be the case in our experiment, since the carrier consists of a train of 100fs pulses, and such time dependence in the carrier leads to strong correlations between different frequency components of optical noise. From equation (46), an improvement in precision beyond the quantum noise limit may be obtained in the case that squeezing ($\Phi < 1$) provides a significant reduction in $\text{Var}(p_\Omega)$.